

Author's response: Review 1 (04.04.2019)

R: Referee's comment

A: Author's response

C: Change in manuscript

(1)

R: The manuscript describes the new development in the capacitively coupled method which was developed for low-frequency measurements. Authors modified the method by including Cole to Cole parameterization. However, for someone not deeply familiar with these methods it hard to follow the manuscript. It was very unclear from reading an abstract: Why is it important to modify low frequency method in first place? What do low frequency methods provide? Why it is important to extend them to wider frequency range? Which additional rate of frequencies does this new modification cover? What type of information do we get by inverting CCR data?

A: We can measure with our method from 1Hz up to 240 kHz, IP works usually in the range of mHz up to 1kHz. The higher frequencies in combination with the high resistivity conditions enable to estimate the resistivity as well as the permittivity of the subsurface. Ice (and snow) has a characteristic relaxation process within our frequency range at around 10kHz, which is what makes the extension in frequency range so important. The Cole-Cole model gives a possibility to fit the spectra of these data. We can determine the 5 Cole-Cole parameters and thereby characterize the subsurface. The modification of the inversion algorithm is necessary because compared to existing IP inversions we need one more parameter.

C: The abstract will be rewritten such that the aim of the study and the issues mentioned above become clearer. Also, sections of the introduction will be rewritten to describe better what information can be provided by other methods, and what is new here what we try to obtain out from our method.

(2)

R: Similarly, in the introduction, authors jump on explaining how by having electrical resistivity and dielectric permittivity is not enough. I suggest to start with explaining why doing ERT measurements is important in the first place? What type of subsurface information do we obtain by using these ERT? Then move to explaining why it is not enough and that having permittivity provides and additional information that is useful for interpretation of subsurface conditions. It is not clear, which subsurface conditions authors are referring to?

A: We agree with the idea of starting from the ERT and then explain the benefits of our method. The subsurface conditions we are focusing on are periglacial areas. The main reason is that the method is sensitive to the presence of water ice, due to the characteristic frequency dependence of electrical permittivity.

However, in this paper we focus on methodological aspects, such as the questions: Is it possible to measure the CCR with our unique equipment in areas of (possible) occurrence of ice/permafrost? How strongly are the data affected by the electrode height? Can we invert our data with the new spectral 2D inversion and are results consistent with the subsurface structure and literature values?

The quantitative estimation of ice content is an ultimate goal of future developments, for which we lay the foundation with this work.

C: We will rewrite several sections of the introduction. First we focus more on the existing studies and methods, starting from ERT and then explaining the role of spectral induced polarization (SIP). We will explain the characteristic relaxation of ice and make clear why our measurement uses these aspects to obtain specific additional information.

(3)

R: First paragraph ends with statement that determination of the ice content is possible with ERT. Is that the overall goal of this work?

A: This might be subject of future work. The statement was intended to point out what could be possible (and was already discussed by several authors). It is not the focus of this work.

C: The focus of the work will be explained more clearly. The introduction will be changed accordingly (see (2)).

(4)

R: P2L10 Why is it usable on the extremely hard surface? Need to better explain it. From the description, I not sure what type subsurface information CCR provides.

A: On hard surface the capacitive coupling gives an advantage over the “normal” coupling with skewers (no drilling or watering of electrodes needed). This is explained in P2 L10-13.

The information are resistivity, permittivity and the characteristic relaxation information given by the other CC parameters (tau, low-frequency permittivity).

C: see (1) (2)

(5)

R: P2L30. OK, the aim of the study is test the application of the newly developed method on the identification of the ground ice.

A: Yes.

C: See above. We will try to make this clear from the beginning.

(6)

R: Shilthorn From the description of the subsurface I conclude that it is a rock. What type of ground ice can exist in the solid rock? Does that rock has fractures that filled with ice? What about ice that might be formed at the ground surface? Does that ice layer is important and was taken into account?

A: The surface under the snow is a layer of limestone (described in the text). Unfortunately, we do not know details, like if its fractured. We do not have a high investigation depth, so just ice in very shallow depth would influence the measurements. But main focus lies on the structural aspects.

C: Will formulate this more precisely and add information.

(7)

R: Lake site Lake was frozen. Is there any information of the ground subsurface? Is it frozen? How deep is the seasonal frost layer? Any information on the percentage of ice within the ground?

A: Unfortunately, there is no further information of the ground subsurface. The measurements were made with the idea to test whether the transition between lake and land is visible in our data. A correlation with geology, or quantitative estimation of ice content, was not a primary goal. Therefore, we can make an assessment of the data only in a qualitative sense.

C: We try to make it clear that we are not aiming at a quantitative correlation with ground properties, but that we consider the qualitative assessment sufficient at this stage.

(8)

R: P6. L10. There some GRP measurements in permafrost regions that estimate ALT (active layer thickness) and soil moisture, and could be used to calculate ice content (e.g. Chen et al., 2016 and Jafarov et al., 2017).

A: We thank for pointing out this papers. Since the estimation of ice content is only an overall goal but not part of this paper, we avoid further discussion of this topic.

C: -

(9)

R: P6.L15 What is relatively high? Do you mean ice lenses wise or massive ice?

A: This statement just means that the existence of ground ice, as in periglacial areas, leads to high resistivity without the distinction between massive or ice lenses. The “relatively” might be misleading.

C: The sentence will be reformulated.

(10)

R: P6.L15-22 lit review and can be moved to the introduction.

A: We agree

C: Will be included in the introduction (see (2)).

(11)

R: P7.L25-30 Does that mean that inversion depends on one parameter (c)?

A: No, that is not the case. We just want to say that the other 4 CC-Parameters can directly be related to a physical context and there exist material-specific literature values. There are values for c as well, but just rare.

C: Sentence P7 L28 f. will be changed.

(12)

R: P8.L23. Figure 4 inversion done with and without determination of height. Where are those two on the plot? I do not see two curves (one for h_0 another for h_{inv})? The legend should be adjusted correspondingly. X-axis, is f an actual frequency or logarithm?

Figure 6. It is not clear which of the Tromso data correspond to the lake ice and which to the ground ice?

A: As written in the figure caption, the two variants of inversion cannot be distinguished from each other and therefore are shown as one line (see legend).

The x-axis is the actual frequency, but shown in logarithmic steps. Axis and the corresponding label are standard, so we are not sure what causes the confusion. At this stage, in fig. 6 there is no distinction between lake site and land site.

C: Fig.4 (same Fig. 5c and d) will be changed that for h_0 and h_{inv} separate curves will be shown, but they will lie on each other.

Fig. 6 will be changed, such that there is a distinction between lake site and land site at Tromso data by using two different colors. This will be explained in the text (P11 L7 ff.).

Concerning the frequency axis, we do not see how to change anything, as we follow common standards.

(13)

R: P12.L16 Why authors decided to use AarhusInv code and not BERT for example? How well does AarhusInv compares to other existing codes? Is this code an open source? If it is, then it would nice to provide a link for the modification implemented in the code. Why did authors choose χ^2 metric? Is that commonly acceptable fitness metric? Why not RMSE or Taylor diagram?

A: Because two of the authors are developers of AarhusInv, working at Aarhus University. Using BERT would cause the same procedure of extending the code for our aims.

AarhusInv is a freeware for non-commercial purposes (<http://hgg.au.dk/software/aarhusinv/>). The code is not open source. The complex impedance is modelled in 2-D solving the Poisson's equation, Fourier transformed in the strike direction, without considering EM effects (Fiandaca et al., 2013), as done for instance in the complex resistivity code cR2 developed by Andrew Binley (<http://www.es.lanccs.ac.uk/people/amb/Freeware/cR2/cR2.htm>).

The data misfit values are expressed in terms of chi values, because the objecting function minimized in the inversion process is the sum of the data and regularization chi values (Fiandaca et al., 2013).

C: We will add information about AarhusInv and the usage of Chi in chapter 4 and 4.3.

(14)

R: P20.L17 'reasonably consistent' ... Is that possible to quantify it (what is the correlation)?

A: Very difficult to quantify because we do not have exact values for resistivity and permittivity from other methods or even better from laboratory analysis. This statement should mean that the determined values fit in the range of literature values of what we know and what we expect from the subsurface at the test sites.

C: Will be formulated more precisely.

(15)

R: Overall, I have been struggling throughout this paper to understand the purpose of this study. What is an ultimate goal of doing this? Is it to get a better measurement of the ground ice? If yes. Are there any ground truth data? How these inversion can be compared with in-situ data? Suggestions: In this current version of the manuscript, methods, results, and literature review are all mixed up together. Think how you can better organize/separate them. Starting from the bigger picture, like knowing ground ice is extremely important for many reasons... In particular, for better understanding of the permafrost thawing rates and consequences. Then introduce the method. Provide a literature review on the existing methods and models. Justify the usage of the current model and talk about how important the current improvements are in terms of better quantifying of the ground ice. In addition, in the description of the site location, it would be extremely useful to know subsurface characteristics/properties. Are there fractures in the rock? How much do you know about subsurface

ground ice at the lake station? Comparing inversely derived ground ice with actual ground ice will be extremely useful. The current version is a good methodological paper and missing emphasis on how this work is important and how it is contributing the current state of science. Addressing these two missing issues will make this paper suitable for the journal like Cryosphere.

A: We appreciate to positive evaluation as a good methodological paper, and we are thankful for the constructive comments. We will try to address the issues and hope that we can bring the paper into a suitable form.

The purpose of the study is to investigate methodological aspects of a new method that can be useful for the investigation of periglacial environments, and demonstrate its feasibility. Therefore, we make an important step towards quantitative usage, such as the estimation of ice content.

The main purpose is not, however, to actually calculate ice content and compare the results with ground truth data. We admit that this would be desirable to have, but it is difficult to obtain in general, and not available for our test sites. We believe that our results are nevertheless important and interesting for a broad readership.

C: We will restructure the abstract and introduction to better describe the purpose of the study. We will also provide a better context of existing methods and research and explain the potential improvement by our method (see (1)(2)(3)). However, instead of a full literature review, we will prefer to refer to a small selection, as the importance of ground ice, and the usefulness of geophysical methods in general, and electrical methods in particular, have already been discussed in textbooks.

There is not much additional information about the field sites (see (6)(7)), but we will try to give a better explanation of what we know and how we can compare the data with existing information.

Author's response: Review 2 (02.05.2019)

R: Referee's comment

A: Author's response

C: Change in manuscript

R: SUMMARY

This paper presents data and modelling results for broadband spectral capacitive resistivity experiments performed in cold regions. The experiments appear sound in design, and the data are novel and very interesting from the perspective of electrical/electromagnetic geophysics and cold-regions research.

A: We appreciate the overall positive evaluation and we thank for the constructive comments.

(1)

R: However, the paper has a few shortcomings. The objectives of the paper are not entirely clear at first. Is the focus on SIP or CR? It becomes clear (I think) that the focus is on cold-regions application of broadband spectral CR. If this is the desired focus, the paper would be made more impactful by including: 1) a review of electrical, IP, SIP, and CR applications to cold regions and permafrost; 2) a clear description of the benefits, limitations, and favourable conditions for broadband spectral CCR, and how these relate to cold regions; and 3) a more thorough analysis of the inversion results in terms of cold-regions ground properties of interest such as water content, ice content and temperature.

A: The CCR (in the spectral way we use it) is actually the method of SIP in a higher frequency range, additionally using the capacitive coupling instead of the "normal" galvanical coupling. Without the capacitive coupling, the method would be similar to Grimm & Stillman (2015) who call it "Broadband SIP" or the "HFIP" (high-frequency IP) from Zorin & Ageev (2017). We focus on CCR as we used it in the field with the logistical advantages and in the terms of the discussed electrode height effect.

C: 1) A review of existing methods and studies of ERT, IP, CCR will be provided in the introduction. We will, however, refer back to textbooks instead of a full literature review, because some of the aspects have already been summarized.

2) Our CCR method will be described more precisely.

3) The analysis of the Inversion results will be described and compared with external information in more detail (p13 ff.). We will not be able to provide an extensive ground-truth comparison, however, because ground truth, for example in terms of ice content, is not available for our test sites. Since the focus of the paper is more on methodological aspects, we hope that this issue is not so critical.

(2)

R: Abstract: Lacks focus on objective and results.

A: We agree that the abstract needs to be rewritten.

C: Abstract will be reformulated to describe objective and results more clearly.

(3)

R: p1,L19: Why? High conductivity material exhibit spectral characteristics as well.

A: It is true that high cond. subsurface exhibits spectral characteristics. But for the determination of the permittivity (in addition to resistivity), lower cond. material is more suitable, because we are limited in frequency range. The reason is, that as lower the conductivity is, the transition to displacement currents and therefore the possible extraction of the permittivity, happens for lower frequencies (e.g. Zorin & Ageev (2017)).

C: The relationship between conductivity and determination of permittivity will become clear in a new section explaining the operating range off CCR (see below).

(4)

R: p.2,L28: What about Routh et al. (1998), Kemna et al. (2000) and several works thereafter?

A: These inversions of IP data works in the way that they invert single frequency data and the in postprocessing integrate all spectral and spatial data, which is the difference to the work of Günther and Martin (2016) and Maurya et al. (2018), who invert all frequencies at the same time. But we agree, that this works should be mentioned in the manuscript.

C: The works with an explanation will be included in the introduction.

(5)

R: p.2,L30: Introduction is somewhat unclear. It starts out focussed on SIP, then CCR, but then states the objective as investigating the field applicability of [spectral] CCR in cold regions. To support the latter, the intro needs a little more background on electrical geophysics and material properties in permafrost and/or glaciology.

A: We agree.

C: The introduction will be reorganized. There will be a review of existing electrical methods and studies before explaining what is new and what is the goal of our method (see (1)). Additionally, the connection to material properties of ice will be made clearer.

(6)

R: eq.1: Although somewhat semantic, I view the low-frequency CCR experiment as responding to the complex conductivity where the imaginary conductivity has a contribution from the real dielectric. Of course, at higher frequency and in the presence of ice, permittivity may be more relevant. However, I do not think that equation 1 should be referred to as representing the "complex permittivity." Consider "effective permittivity" which has a contribution from the imaginary conductivity. The distinction is important because the true dielectric permittivity is what results in wave propagation in Maxwell's equations, not the imaginary conductivity. Furthermore, to talk only of displacement currents denies the possibility of IP-type currents which may dominate at lower frequency.

A: We agree, and actually tried to express this by using the term "effective value" on p5., l.11.

C: We will now explicitly call eq. (1) "effective permittivity", and will also add a few lines on conduction and displacement currents, referring to the overview given by Loewer et al. (2017).

(7)

R: p.6,L4: You say the "conduction current" is in-phase, but then you say that IP is concerned with the conduction current part of the impedance. You need to be clearer on the distinction between the real conductivity (conduction current), the imaginary

conductivity (IP current), and the real permittivity (displacement current).

eq.4: Again, consider noting that any IP effect will be wrapped up in here as $\epsilon_{\text{eff}} = \epsilon R + \sigma/\omega$.

A: see (6)

C: We will introduce that in a short paragraph in chapter 3 (see (6)).

(8)

R: p.7,L8: The height effect is also discussed by Wang et al. (2016) but in a shady pseudojournal. The authors could decide if it warrants consideration.

A: Thank you for pointing this out to us. We agree that it is relevant for our work.

C: The reference will be included.

(9)

R: p.8,L3: You say the inversion is frequency dependent, but then go on to say that the system response is controlled by geometry, not frequency. Clarify.

A: The statement refers to the fact that we work in the range of “geometric sounding” (same as ERT) and so we do not have a frequency sounding (as e.g. RMT); See (10)

C: see (10)

(10)

R: p.8,L5: You need to thoroughly describe the “operating range” of CCR with respect to treatment of the data for the single site inversion and the 2D inversion. Application of a 2D resistivity inversion (with geometry-based sensitivity) requires low-induction number conditions (which actually appears to be violated for some of your lower frequency-resistivity combinations). Does the single-site inversion require LIN conditions? What about wave effects? For some of the high frequency-resistivity pairs encountered, quasistatic conditions are violated and a true permittivity will result in wave propagation. This should not(?) affect CC model fits, but it should(?) affect the 2D inversions using a resistivity-type sensitivity function.

A: The method of CCR operates in the physical range of “geometric sounding” (GS), which indeed requires LIN conditions to be fulfilled. We do not agree, however, that these are violated for some of our data (see more detailed explanation below). Quasistatic conditions, however, are not necessary, because it is the wavenumber that determines which physical process dominates. The detailed explanation is as follows:

The physical boundaries are given by the effects of electromagnetic induction (EMI) and wave propagation (WP). This consideration of the three processes is described in Weidelt (1997) and the “parameter range” refers to the frequency f , the spatial scale a (i.e. distance between transmitter and receiver), electrical conductivity and permittivity.

The equation that allows to compare the processes is: $\gamma^2 = \frac{4\pi}{a^2} + \frac{2i}{\delta^2} - \frac{4\pi}{\lambda^2} = GS + EMI - WP$, where the process corresponding to the largest term will dominate, and the other terms may be negligible, depending on their magnitude.

Skin depth: $\delta = \frac{1}{\sqrt{\pi f \mu \frac{1}{\rho}}}$; wave length $\lambda = \frac{2\pi}{\omega \sqrt{\epsilon\mu}}$

If we calculate this as a worst-case for our maximum frequency 240 kHz, a smallest resistivity (lowest conductivity) of 100 Ohmm and a spatial length of 10 m, we are still clearly in the range of GS. (GS=4; EMI = 0.02; WP=8e-5)

So we think that there is no violation neither to induction effects nor to wave propagation. For the presented measurements, we always have low-induction numbers and therefore can neglect possible resulting problems in terms of the inversion.

Anyway, we agree that this point has to be made clearer in the manuscript.

C: We will describe the operating range and the topic of GS, EMI and WP in a new section within chapter 3.

(11)

R: p8,L6: "Induction effects" would typically be understood to mean inductive source effects of current-carrying cables. You don't have these. So, do you mean magnetic coupling as described by McNeill?

A: Yes, we (as in Fiandaca (2018)) mean the electromagnetic induction effects.

C: Will be described more deeply (see (10)), and we will use more precise terminology).

(12)

R: p.13,L25: Well, the dielectric constants for rock and snow are both around 3-5, so...

A: Yes, this is the reason why the values are so close and material is difficult to distinguish.

C: We will include this in the statement.

(13)

R: p.13,L32: Snow cover typically inhibits frozen ground.

A: We agree, the sentence is unclear and actually not necessary for the further discussion.

C: Will change the statement.

(14)

R: Table 1: Add water. More discussion is required in comparing recovered values to expected material properties.

A: The discussion can be done in more detail and by including water in table 1 and the discussion.

C: Will add water in table 1 and deepen the discussion when comparing literature values with the inversion results for the test sites.

(15)

R: p.15,L5: In comparing to literature values, what about the observations by Weigand and Kemna (2016) that SIP model parameters obtained from a CC model are biased? Is this alleviated by having c as a free parameter and/or by having 19 points in the spectrum?

A: We thank for pointing this out and agree that this should be included in the text. Yes, we think that the fact of having c as free parameter (see below (18)) and having the high density of 19 frequency measurements in the range of estimated τ alleviate the effect of bad determined CC parameters. The inverted τ -value are in the expected range of relaxation for ice and snow, what strengthen our assumption.

C: Observations about the resolution of CC-Parameters (e.g. Weigand and Kemna, 2016) will be included and discussed in the context of our results. (chapter 4.1)

(16)

R: Fig.8: Use same scales as Fig.7. Are some of the observed differences attributable to height effects or breakdown of LIN conditions?

A: As explained there should be no breakdown of LIN conditions (see (10)). Moreover the height effects in our cases should be too small to influence the 2D inversion, as shown in fig. 6 and discussion. The differences have to be due to the fact that figure 8 is a pseudosection, whereas figure 7 is a 2-D inversion result. We actually had devoted an extra paragraph to this discussion (p. 13, l. 10ff).

C: Since spatial variation in pseudosections is always smoother compared to inversion results, using the same scales would result in loss of information. Therefore, we would prefer to leave the scales as they are. Instead, we try to clarify the discussion of pseudosection and inversion result.

(17)

R: p.18,L5: Why is the DC permittivity so (unreasonably) high?

A: The values are higher than expected comparing with literature values. Nevertheless, LF values of permittivity for natural water, specially with high salinity (as it is in the lake), can be very high (Seshadri et al, 2008). On the other hand an overestimation may be caused by the measured low frequency values (see e.g. Zorin and Ageev (2017)).

C: The role of epsDC and the high inversion results of Tromso data will be discussed in more detail.

(18)

R: p.18,L11: Is there any benefit to setting c constant (i.e., choosing a decomposition for the CC model). Is it reasonable for c to show so much variability? Is it highly sensitive, and if so, is it just absorbing error in the inversion?

A: We did some inversion tests with constant c. It shows that a constant c cannot fit the data of all the different spectra. We think that the different subsurface materials and conditions explain the variability of c and justify the use as free parameter.

C: Will be mentioned in the text.

(19)

R: p.18,L19: Actually, the LF permittivity of water is around 80, but you need to get up to 1010 to 1012 Hz before it drops to around 3.

A: We have to make this clear that the relaxation of water refers to higher frequencies and the value of 80 is the low-frequency value.

C: Will be changed in the text and described in context of adding literature values of water in table 1 (see (14)).

(20)

R: Figure 10: a) Use dash and solid. b) What is the distinction between black and purple lines?

A: b) The distinction is measured (purple) and inverted (black)

C: a) will be changed b) will be added in the figure caption

New References: M. Loewer, T. Günther, J. Igel, S. Kruschwitz, T. Martin and N. Wagner: Ultra-broad-band electrical spectroscopy of soils and sediments – a combined permittivity and conductivity model; Geophysical Journal International 210, 1360-1373; 2017

List of changes

(pages and lines correspond to the new manuscript)

Abstract (p.1): rewritten

Chapter 1 - Introduction (p.2-4): rewritten

Chapter 2.1/2.2 (p.4-5): additional information about the test sites (Schilthorn and Tromso) added

Chapter 3 – Basics of the method (p.6 L.12 ff.): additional information about the electrical parameters (resistivity and permittivity) and renamed “effective permittivity”

Chapter 3 (p.7 L.23 ff.): section transferred to the introduction

Chapter 3.1 (p.8 L.31): adjusted statement

Chapter 3.2 – Operating range (p.9-10): a new chapter is added; description about the operating range including discussion about electromagnetic induction effects.

Chapter 3.3 (p.10 L.22 ff.): adjusted statement; transferred to new chapter 3.2

Fig 4+5 (p.11 and 13): h_0 and h_{Inv} are shown in separate curves for all plots

Fig 6 (p.14): Tromso data are splitted in Lake and Shore data; corresponding changes in the text description

Chapter 4 (p.16 L.23): added information about AarhusInv

Chapter 4.1 (p.17 L.9 ff.): new section discussing the resolution of CC-Parameters (e.g. Weigand&Kemna, 2016) and the relaxation exponent c

Chapter 4.1 (p.19 L.5 ff.): changed statement about possible ice cover

Chapter 4.1 (p.19 L.21 ff.): added section about electrical properties of water (added also in Table 1)

Chapter 4.1 (p.19 L.28 ff.): discussion about Fig. 7 adjusted

Table 1: water added

Chapter 4.1 (p.20 L.10 ff.): changed statement about comparison of Fig. 7 and 8

Chapter 4.2 (p.23 L.19 ff.): discussion about electrical properties including lake water characteristics

Chapter 4.3 (p.23 L.29 ff.): statement about the data misfit χ

Fig 10: a) used solid and dashed lines; figure caption

Fig 11: adjusted figure caption

Chapter 5 (p.26 L.5): changed statement about consistence of results

Two-dimensional Inversion of wideband spectral data from the Capacitively Coupled Resistivity method - First Applications in periglacial environments

Jan Mudler¹, Andreas Hördt¹, Anita Przyklenk¹, Gianluca Fiandaca², Pradip Kumar Maurya², and Christian Hauck³

¹Technische Universität Braunschweig, Institut für Geophysik und extraterrestrische Physik, Braunschweig, Germany

²Aarhus University, Department of Geoscience, Hydrogeophysics Group, Aarhus, Denmark

³University of Fribourg, Department of Geosciences, Fribourg, Switzerland

Correspondence: Jan Mudler (j.mudler@tu-bs.de)

Abstract. ~~The Capacitively Coupled Resistivity (CCR) method determines the electrical resistivity and permittivity by analysing the spectra of magnitude and phase shift of the electrical impedance. The CCR is well suited for the application in cryospheric and periglacial areas, because these areas provide the required physical conditions and logistical advantages of the method regarding the problems of coupling on highly resistive grounds and in some cases hard surfaces. Since DC resistivity method~~
5 ~~is a common tool in periglacial research, because it can delineate zones of large resistivities, which are often associated with frozen water. The interpretation can be ambiguous, however, because large resistivities may also have other causes, like solid dry rock. One possibility to reduce the ambiguity is to measure the frequency-dependent resistivity. At low frequencies (<100 Hz) the corresponding method is called induced polarization, which has also been used in periglacial environments. For the detection and possibly quantification of water ice, a higher frequency range, between 100 Hz and 100 kHz, may be particularly~~
10 ~~interesting, because in that range, the electrical properties of ice and frozen material have a strong frequency dependence, broad spectral measurements can deliver complementary information compared to conventional low-frequency techniques. For the inversion of the data, we modified an existing 2-D inversion code originally developed for low-frequency Induced Polarization data by including a Cole-Cole parametrization of electrical permittivity. We discuss the application of the code and particular aspects related to capacitively coupled measurements using data from two~~ water ice exhibit a characteristic behavior.
15 In addition, the large frequencies allow a capacitive coupling of the electrodes, which may have logistical advantages. The capacitively coupled resistivity (CCR) method tries to combine these logistical advantages with the potential scientific benefit of reduced ambiguity.

In this paper, we discuss CCR data obtained at two field sites with cryospheric influence: the Schilthorn massif in the Swiss Alps and the frozen lake Prestvannet in the northern part of Norway. ~~We~~ One objective is to add examples to the literature
20 where the method is assessed in different conditions. Our results agree reasonably well with known subsurface structure: At the Prestvannet site, the transition from a frozen lake to the land is clearly visible in the inversion results, whereas at the Schilthorn site, the boundary between a snow cover and the bedrock below can nicely be delineated. In both cases, the electrical parameters are consistent with those expected from literature.

The second objective is to discuss useful methodological advancements: First, we investigate the effect of capacitive sensor height above the surface and corroborate the assumption that it is negligible for highly resistive conditions. The first results agree reasonably well with known subsurface structure and measurements reported in the literature. We conclude that a spectral For the inversion of the data, we modified an existing 2-D inversion with a Cole-Cole parametrization of permittivity is a feasible tool to invert CCR data in periglacial environments code originally developed for low-frequency Induced Polarization data by including a parametrization of electrical permittivity. The new inversion code allows to extract electrical parameters that may be directly compared with literature values, which was previously not possible.

Copyright statement. TEXT

1 Introduction

Spectral electrical measurements over a wide frequency range allow the determination of the electrical resistivity ρ as well as the relative dielectric permittivity ϵ_r . The determination of the permittivity as an additional parameter can result in complementary information compared to conventional electrical measurements, which is useful for the interpretation of the subsurface conditions. Areas of low electrical conductivity are particularly suitable for the determination of both parameters. Ice or frozen soils, such as permafrost, are potential fields of application, since they exhibit a characteristic frequency dependence of the Electrical resistivity measurements determine electrical properties of the subsurface. They can support the investigation in periglacial environments, because they provide information on regions below the surface, otherwise only accessible by drilling. The DC resistivity method, called electrical resistivity tomography (ERT) if used to create vertical sections, is most useful to “detect, localize and characterise structures containing frozen material” (Hauck and Kneisel, 2008). The reason is that electrical resistivity dramatically increases when temperature falls below the freezing point of water. Therefore, ERT is “maybe the most universally applicable method in permafrost related mountain environments” (Hauck and Kneisel, 2008). However, the interpretation of ERT data may be ambiguous, because the huge electrical resistivities associated with frozen material can also be due to dry, unfrozen rock, or to air in the pore spaces. In particular, when quantitative estimates, such as ice content, are desired, complementary information is usually required. One possibility is to combine ERT with other geophysical methods, such as ground penetrating radar, or seismics (Hauck et al., 2011). Another idea is to measure the frequency-dependence of electrical impedance (Petrenko and Whitworth, 2002). In principle, the determination of the ice content in the subsurface is possible from the results of wide-band electrical measurements (?). resistivity, along with the DC resistivity itself. In that case, the method is called induced polarisation (IP), or spectral induced polarisation (SIP), when measurements are made over a broad frequency range. The method has traditionally been used for a variety of applications, such as mineral exploration and the assessment of hydraulic properties of sediments, amongst others (Kemna et al., 2012). Applications in periglacial environments are sparse; a recent example of the investigation of a rock glacier is described in (Duvillard et al., 2018).

Many laboratory studies for the characterization of samples of frozen material were carried out (Olhoeft, 1977; Seshadri et al., 2008; Grimm et al., 2015). The first spectral measurements on ice and permafrost at the field scale have been performed by Grimm and Stillman (2015) for a characterization of ice. Furthermore, the successful determination of the two electrical parameters At the field scale, SIP measurements are typically made at relatively low frequencies (say <100 Hz). At higher frequencies (roughly > 100 Hz), field data are less frequently measured, one reason being that electromagnetic induction (EMI) may inhibit the determination of frequency-dependent electrical properties. In periglacial environments, where large resistivities are typically encountered, EMI is much less important, and the determination of electrical properties at the field scale was demonstrated by Przyklenk et al. (2016), using the method of Capacitively Coupled Resistivity (CCR). In contrast to galvanic coupling by skewers, in the case of CCR plates or cables lying on the ground are used, which are galvanically decoupled from the subsurface and guarantee purely capacitively coupling to the ground. This procedure may have several advantages under certain conditions. On the one hand, this method is non-invasive and usable on extremely hard surfaces, such as rock or ice, on which it is hardly possible to work with skewers and often only by influencing the structure of the subsurface. Likewise, with the help of capacitive coupling, a coupling can be achieved even on subsoils of high resistivity (Hördt et al., 2013), on which galvanic coupling due to high contact resistivity is not possible, or only by special efforts at the electrodes. might be feasible, as will be discussed further below.

Whereas at low frequencies, electrical properties are normally expressed by the imaginary conductivity (Kemna et al., 2012), electrical permittivity is often being used at higher frequencies, (e.g. Stillman et al., 2010). When using complex numbers, the use of conductivity or permittivity is mathematically equivalent, but since the frequency dependence is caused by different physical processes in different frequency ranges, it is common to use permittivity for higher frequencies.

The frequency range >100 Hz up to several 100 kHz is particularly interesting for periglacial processes, because the permittivity of water ice exhibits a characteristic frequency-dependence in that range (Petrenko and Whitworth, 2002). A number of laboratory studies exists that investigate permittivity of natural material including ice (Olhoeft, 1977; Seshadri et al., 2008; Grimm et al., 2015; Murton et al., 2004), suggesting the idea that ice content might even be determined quantitatively (Bittelli et al., 2004). Therefore, if permittivity could be measured at the field scale, a unique piece of information would be contributed that can help to reduce the ambiguity that exists when only DC resistivity is measured.

The usage of relatively high frequencies can help to overcome another major problem associated with electrical measurements in periglacial environments: the coupling between the electrodes and the often hard and very resistive surface (Hauck and Kneisel, 2008). At large frequencies, capacitive coupling becomes feasible. Instead of skewers, plate electrodes may be used. They form a capacitor with the ground, and allow contact-free injection of current even for extremely resistive surfaces (Hördt et al., 2013).

In that case, the method may be considered an extension of high-frequency SIP, called capacitively coupled resistivity (CCR). The CCR method is therefore not just useful for geophysical exploration on ice, but also for space missions (Grard, 1990; Grard and Tabbagh, 1991) and has originally been suggested for applications on space missions (Grard, 1990; Grard and Tabbagh, 1991), where the conditions (large resistivities, difficult electrode coupling) may be similar to those in periglacial environments. Besides application in space (Seidensticker et al., 2007), devices have been developed for investigations in urban areas such as facades (Souf-faché et al., 2010) or roads (Dashevsky et al., 2005; Flageul et al., 2013) where prototypes were already used. Using capacitive

coupling to the ground may be challenging, especially due to the sensor height effect, caused by effective height between the electrodes and the underlying subsurface, as well as archeological sites (Tabbagh et al., 1993) and environmental problems (Kuras et al., 2007).

The first high-frequency SIP measurements at the field scale in periglacial environments were carried out by Grimm and Stillman (2015)

5 , who used the method for a characterisation of subsurface ice. Przyklenk et al. (2016) discuss data from CCR measurements using data acquired on an ice layer at Zugspitze mountain, and develop an inversion scheme based on a homogeneous halfspace assumption. This could strongly influence the measurements and has to be considered (Kuras et al., 2006; Hördt et al., 2013).

Many studies which used the CCR method only measured the magnitude of the impedance at a discrete frequency and used the method just like conventional resistivity measurements (Tabbagh et al., 1993; Kuras et al., 2007; Hauck and Kneisel, 2006). In

10 order to be able to determine both parameters ρ and ϵ_T , additional measurements of the phase shift are required, which have to be carefully designed to avoid electromagnetic disturbances (Przyklenk et al., 2016). By measuring the values of amplitude and phase shift over a broad frequency range, it is possible to obtain the dielectric relaxation of the ground material. Based

on a Cole-Cole parametrization of dielectric relaxation (Cole and Cole, 1941), an inversion for spectral measurements of CCR at a single point using a homogeneous halfspace assumption was suggested by Przyklenk et al. (2016). Although the

15 concept of obtaining high-frequency SIP data using CCR may be considered proven, there is still little experience with field data, and several open questions on the applicability remain. One aspect is the sensor height effect: a distortion of the data arising from electrodes being in a finite distance from the ground. The effect has been investigated both theoretically and experimentally (Kuras et al., 2006; Wang et al., 2016), and there are indications that it can be neglected in periglacial

applications characterized by large resistivities (Przyklenk et al., 2016). However, the effect depends on the specific conditions

20 in each survey area, and there is little practical experience.

For the investigation of larger areas and depth, it is favorable to analyse data by a two- or even three-dimensional. A second aspect not fully solved is the inversion. This is common for most geophysical methods, while for frequency-dependent

measurements, existing Przyklenk et al. (2016) used a so-called single site inversion that treats each 4-point measurement individually assuming a homogeneous halfspace, and inverts only the spectral behaviour. This was justified by the homogeneous

25 subsurface and the small spatial coverage of that data set. Grimm and Stillman (2015) investigated several methods of 2-D inversions for conventional Spectral Induced Polarization (SIP) (Günther and Martin, 2016; Maurya et al., 2018) became

available only recently. inversion in order to produce a vertical cross section. The challenge was that existing IP inversion codes, such as developed by Routh et al. (1998) and Kemna et al. (2000) were only able to invert single frequency data, and

postprocessing is required to integrate all spectral and spatial data. Grimm and Stillman (2015) discuss some difficulties they

30 encountered, which they finally circumvented using the time-lapse feature of RES2DINV, a widely used 2-D inversion code for DC resistivity and IP data (Loke and Barker, 1996). Recently, 2-D inversion codes have become available which are able to invert all frequencies and spatial data points at the same time (Günther and Martin, 2016; Maurya et al., 2018).

The aim of the present study is to investigate the applicability of the CCR method at the field scale in areas of surface (e.g. lake ice) and subsurface (permafrost) ice occurrences. Two case histories will be discussed. Here, we discuss two case histories

35 of CCR applications in periglacial environments, one from the Schilthorn massif in the Swiss Alps and the other one from the

frozen lake Prestvannet in the northern part of Norway. ~~We modified the~~ Besides the general usefulness of gaining experience with CCR field applications and extending the sparse data set existing in the literature, we focus on two aspects. For the 2-D inversion, we modified the SIP inversion code ~~in~~-AarhusInv (Auken et al., 2014), an inversion tool for various geophysical methods, to consider the ~~frequency-dependent permittivity in terms of a permittivity-Cole-Cole model, frequency-dependence~~ and apply the code to the data of our two test sites. We also investigate the potential effect of electrode height and show that it is negligible in both cases.

The results of the 2-D inversion will be compared with existing knowledge about the subsurface stratifications and materials. ~~We discuss the advantages of the determination of both electrical parameters and their potential for the interpretation~~ Although a quantitative assessment of the parameters is difficult because of the sparse availability of additional information, we show that the results are at least not implausible. The new inversion code is suitable for field data and constitutes one step forward towards the ultimate goal: reducing the ambiguity in the interpretation of resistivity data and maybe provide quantitative information, such as ice content.

2 Measurements and test sites

For the application of CCR, we focus on the cryosphere (i.e. ice, snow, permafrost), where the logistic advantages of the capacitive coupling are given in terms of highly resistive ground and in some cases hard surfaces (e.g. ice or frozen ground). The method enables the ability to measure directly on snow and ice. The measurements were carried out using the Chameleon equipment from Radic Research, which is ~~specially~~-specifically designed for the application of broadband measurements of the electrical impedance (Radić, 2013; Przyklenk et al., 2016). The prototype device uses a 4-electrode array. Therefore, two-dimensional measurements along a profile and in depth are achieved by gradually shifting and enlarging the array. It is possible to measure in a range from ~~1 Hz up to 240 kHz~~ 1 Hz up to 240 kHz at 19 discrete frequencies. The results are the spectral values of the magnitude $|Z(f)|$ and the phase shift $\varphi(f)$ of the impedance. Wenner- and dipole-dipole configurations were used.

2.1 Schilthorn

The survey was carried out in July 2016 on the Schilthorn massif, in the Bernese Alps, Switzerland. There is occurrence of alpine permafrost in the area ~~, as documented by Hilbich et al. (2008) and Imhof et al. (2000)~~ (e.g. Hilbich et al., 2008; Scherler et al., 2010). Figure 1 illustrates the geographical location. Panel B shows the area from village Mürren up to the summit Schilthorn. The mountain station Birg is in between and can be reached by a cable car. The position of the selected profile B-SCH, north of Birg, at an altitude of about 2700 m a.s.l. and with a length of 27 meters, is shown in Fig. 1C. The surface in this area mostly consists of rock, which is covered with snow most parts of the year (i.e. October-July). On the summit area, the ground material is described as weathered. The occurrence of an ice layer under the snow is possible, as modelled by Scherler et al. (2010).

The photograph in Fig. 2 shows an example of the equipment layout in the field. The plate electrodes, which are covered with capton foil for galvanic decoupling, were arranged in a profile line. They are connected by cables through a probe and a remote

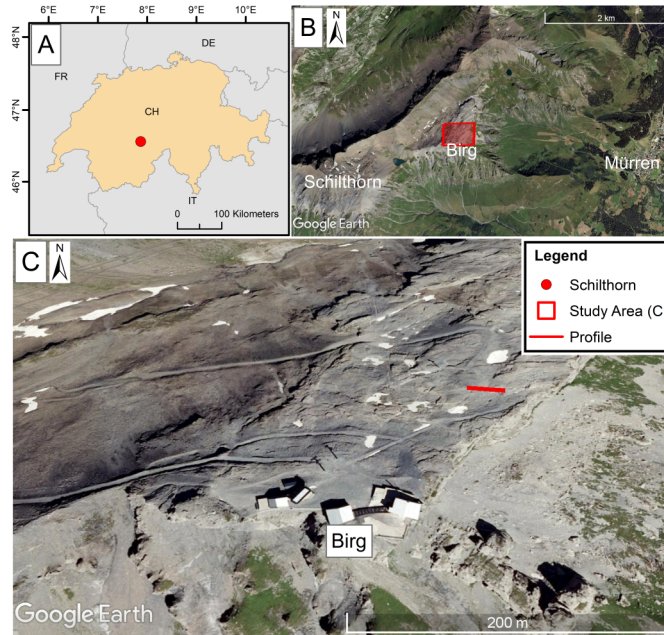


Figure 1. Geographical maps of the Schilthorn area. Panel A shows the location in Switzerland. In panel B the Schilthorn area with the village Mürren, the mountain station Birg and the summit is shown. The area around Birg, where the measurements took place is shown in panel C, including location of profile B-SCH.

unit to the base unit (Przyklenk et al., 2016), which controls the measurements. The surface at the time of the measurements was covered by a layer of snow, which was frozen on the top. The depth of this snow layer was separately measured every two meters using a dipstick for later validation of the results. Measurements were done along the profile in a dipole-dipole configuration ($a = 1$ m) for several electrode spacings ($n = 1 - 6$). They were not carried out with the same electrode spacing throughout the profile. Measurements with wider electrode spacing and corresponding larger penetration depth were carried out only on the first half of the profile.

2.2 Tromsø

The measurements in Norway were done in 2015 on the frozen lake Prestvannet near the town of Tromsø. Figure 3 shows the geographical position of the area and the test site. In Fig. 3B, a part of the peninsula Tromsøya, with the city Tromsø and the lake is are visible. Lake Prestvannet covers an area of about 10 ha, has a maximum depth of 4 meters and is covered by ice most of the year (Stabbel, 1985). Although no quantitative statement is made, investigations of the lake water qualitatively indicate a high salinity (<https://memim.com/prestvannet.html>). The part of the lake, where the test site is located, is shown in panel C, including the profile, which has an extension of 33 meters length and crosses the shore of the lake. The shore was covered with a layer of snow, the lake itself was frozen, and measurements took place directly on the lake ice. Starting the profile on the lake and ending at the shore, the transition to the lake surface is at about profile coordinate 20.5 m.



Figure 2. Photograph of the measurements at profile B-SCH (Schilthorn area) in July 2016 with the Chameleon measurement device. The four plate electrodes are lying in line on the snow surface. The larger yellow box is the base unit which is connected by cables to the electrodes with the cubic grey remote units in between.

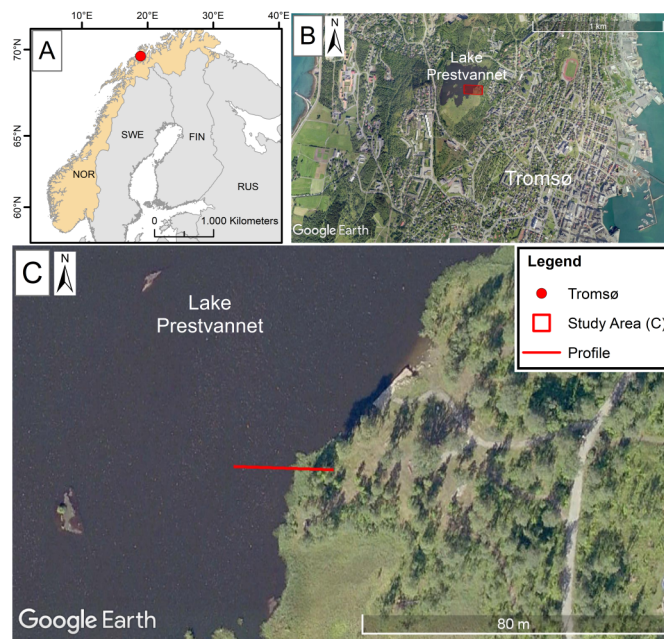


Figure 3. Geographical Maps of Lake Prestvannet. The location in the northern part of Norway is shown in part A by the red dot. The lake is located on the peninsula Tromsøya, presented in panel B, close to the city Tromsø. A detailed view of the test site is given in panel C, showing the profile crossing the boundary from the lake to the shore.

The measurements were done with a fixed electrode spacing in Wenner configuration ($a = 1.5\text{ m}$) to investigate differences in the measured data due to the sub-vertical lake-shore-boundary. The penetration depth of the measurements has therefore a maximum of 1.5 m (Militzer and Weber, 1985). Additional measurements indicated that the boundary to the liquid water was at a minimum of 4 m depth, below the penetration depth of the data.

5 3 Basics of the Capacitively Coupled Resistivity Method

When a time-varying current is injected into the ground, two different physical mechanisms are stimulated: the conduction current associated with the electrical resistivity, and the displacement current controlled by the electrical permittivity. The response of the material contains a combination of these two mechanisms, which can be measured as the impedance. Consequently, it is possible to define ~~an effective~~ a complex value named the ~~complex effective~~ conductivity, respectively the ~~complex effective~~ permittivity ε^* , which combines the conduction and polarization properties, as:

$$\varepsilon^*(\rho, \varepsilon_r, \omega) = \varepsilon_0 \varepsilon_r + \frac{1}{i\omega\rho}, \quad (1)$$

where i is the imaginary unit, ε_0 the permittivity of the vacuum and ω the angular frequency. ~~Note, that In the most general form, both~~ the electrical resistivity ρ and the relative electrical permittivity ε_r are considered as real values. may be considered complex and frequency-dependent (Loewer et al., 2017). However, since this general description is redundant, it is a matter of choice or convention whether frequency-dependence is expressed by resistivity, respectively conductivity, or permittivity. In the low-frequency range used by conventional SIP, frequency-dependence is commonly expressed by an imaginary conductivity (e.g. Maurya et al., 2018), whereas at higher frequencies permittivity is normally used (e.g. Stillman et al., 2010). Here, we choose to express our results in terms of frequency-dependent permittivity, assuming resistivity a real, constant value, as will be detailed below.

The three variable quantities, i.e. ω , ρ and ε_r determine in mutual dependence the weighting of the two current components. The injected current and the measured voltage are in-phase for the proportion of conduction current and shifted by -90° for the displacement current component.

Most geophysical methods working with time-varying electric fields focus on one of the two mechanisms by defining a chosen frequency range and neglect the other part. The ratio of the proportions of both current mechanisms gives an estimation for the physical regime of the measurements. Geophysical methods such as Induced Polarization (IP) or Magnetotellurics (MT) (Telford et al., 1990) work in a rather low frequency range where the conduction current dominates the signal of the impedance. The Ground Penetrating Radar (GPR), on the other hand, works at very high frequencies and focuses on the displacement current, determining the permittivity (Zorin and Ageev, 2017). Our aim is to measure in an intermediate frequency range where both current mechanisms are relevant in order to determine both electrical parameters (see Eq. (1)). In order to ensure this in our given frequency range, the subsurface materials have to exhibit relatively high resistivities and permittivities. The condition may be calculated based on the loss tangent (Przyklenk et al., 2016). Typically, for our frequency range the resistivity has to

be greater than $1000\Omega\text{m}$. The needed conditions are particularly prevalent in periglacial areas, ~~where~~ with the occurrence of ground ice ~~can be relatively high~~ (Arenson et al., 2015; Hauck and Kneisel, 2006).

~~In the early 1990s, the theory of a capacitively coupled quadrupolar array was first proposed by Grard (1990) and later deepened by Kuras et al. (2006). In the following years devices were developed and used in the field (Grard and Tabbagh, 1991; Tabbagh et al., 1993;~~

5 ~~The assumption is that the galvanically decoupled electrodes in the form of plates, disks or wires are lying on the interface between two media. In most cases, and in the following considerations, it is the interface between air and ground. The theory leads to a~~ The description of the complex impedance ~~as follows, where the form suggested by Kuras et al. (2006) was by~~ Kuras et al. (2006), modified by Przyklenk et al. (2016) in order to use the unmodified geometry factor K , known from DC resistivity, is:

10

$$Z(\omega, \rho, \varepsilon_r, h) = \frac{1}{2i\omega\varepsilon_0 K} [1 - \alpha(\rho, \varepsilon_r)H(h)], \quad (2)$$

where the reflection factor α contains both electrical parameters of the subsurface.

Special attention is given to the height factor $H(h)$. It depends on the geometry factor K and a vertical geometry factor, which
 15 describes the height of the capacitively coupled sensors. In the case of an ideal contact of the electrodes to the ground, the height h becomes zero and the resulting height factor H becomes one. Thus, the electrical parameters for each frequency can be determined directly from the real and imaginary part of the impedance (Przyklenk et al., 2016):

$$\rho = \frac{K}{\text{Re}(Z^{-1})} \quad (3)$$

20

$$\varepsilon_r = \frac{\text{Im}(Z^{-1})}{K\omega\varepsilon_0} - 1 \quad (4)$$

The challenge is that the electrodes, especially in the case of plates or discs usually do not rest over their entire surface on the ground. Rather, with a slight unevenness of the ground, a contact of the electrodes to the ground is ensured only at a few points.

25 This results in a mean non-zero height h of the electrode surface over the ground, which however can hardly be measured directly. The height dependence was already discussed by a few authors (Kuras et al., 2006; Przyklenk et al., 2016). Even small heights in the range of micrometers can cause large differences in the measured impedance, but this dependence becomes weaker as resistivity and permittivity increase.

3.1 Cole-Cole Model

30 The electrical permittivity and the resistivity are not constant values in most cases but vary with frequency. Polarizable materials, e.g. water-saturated sediments or mineralized rocks exhibit a strong frequency dependence of electrical parameters (Zorin and Ageev, 2017). This is especially true in periglacial areas, for materials with pure ice or large ice contents

(Petrenko and Whitworth, 2002; ?; Stillman et al., 2010)(Petrenko and Whitworth, 2002; Bittelli et al., 2004; Stillman et al., 2010)

. Przyklenk et al. (2016) investigated several parametrizations of the frequency-dependence of resistivity and permittivity. They suggest the use of the Cole-Cole Model (CCM) (Cole and Cole, 1941), which provides reasonable results when fitting the spectral data of CCR measurements. For variable data with more spectral shape, a dual CCM, corresponding to a model of a two-component mixture, might be necessary for the evaluation of the impedance spectrum. For our studies, we decided to use the single CCM, which includes just one material, because it can fit our data with a minimum number of parameters. For the relative complex permittivity, the single Cole-Cole Model is expressed by:

$$\epsilon_r^* = \epsilon_{HF} + \frac{\epsilon_{DC} - \epsilon_{HF}}{1 + (i\omega\tau)^c} + \frac{1}{i\omega\epsilon_0\rho_{DC}}. \quad (5)$$

10

The description of the frequency dependence of the electrical parameters is based on five Cole-Cole parameters: the DC resistivity ρ_{DC} , a low-frequency limit ϵ_{DC} , a high-frequency limit ϵ_{HF} , which is referred in the literature as the dielectric constant, the relaxation time τ and the relaxation exponent c . The positive relaxation exponent can range up to a maximum value of one, for which the model simplifies to the Debye Model (Petrenko and Whitworth, 2002). ~~Except for the relaxation exponent, all values~~ The parameters are directly related to a physical context. Thus, they are material-specific parameters for which ranges of literature values are known, that can be used for a discussion of the inversion results.

15

3.2 Single Site Inversion~~The single site inversion was the primary method used in Przyklenk et al. (2016). The data of each measured 4-point array is inverted separately, i.e. without influence of other measurements. Thus, this spectral inversion contains a dependence on frequency, but not on space. In this context it is important to note that under the physical conditions of the CCR method, Operating range~~

20

There is a parameter range in which CCR method is feasible in the sense that the underlying assumptions are fulfilled and the physical process that is used to determine the spectral behaviour of permittivity and conductivity actually dominates. The term "parameter range" refers to the frequency, the spatial scale (i.e. distance between transmitter and receiver), and electrical conductivity and permittivity. The CCR method operates in the propagation of the electromagnetic fields is just limited by the geometry but not by the used frequency (Weidelt, 1997). Induction effects can be neglected, „geometric sounding“ range, where the investigated volume and in particular the penetration depth depend only on the location and the distance between transmitter and receiver. This is the same condition that applies to the ERT method.

25

The two processes that need to be investigated because they may limit the operating range of CCR are electromagnetic induction (EMI) and wave propagation. Electromagnetic induction currents are caused by the time-varying magnetic fields which always co-exist with electric fields. Several methods are based on EMI, which is particularly important if the conductivity is large. Wave propagation is the basis of ground penetrating radar (GPR) methods, and is particularly important for very large frequencies. For an assessment of the relative importance of the processes we use the consideration by Weidelt (1997)), who compares the wave lengths (or their inverse, the wavenumbers) of the three processes with each other. The wave length of EMI is equal to

30

the skin depth, given by

$$\delta = \sqrt{\frac{2\rho}{\omega\mu}} \quad (6)$$

- 5 where μ is the magnetic permeability, where in this context it is sufficient to use the vacuum value, which is $\mu_0 = 4\pi \times 10^{-7} \frac{Vs}{Am}$. The wave length of wave propagation is given by

$$\lambda = \frac{2\pi}{\omega\sqrt{\epsilon\mu}} \quad (7)$$

- 10 For geometric sounding, the signal is composed of many different wavelengths, but for an estimate of the relative importance of the processes, it is feasible to use an appropriate measure of the spatial scale of the electrode configuration (i.e. the electrode distance a for Wenner configuration), as the dominant wave length. The equation that allows to compare the three processes is (Weidelt, 1997):

$$15 \quad \gamma^2 = \frac{4\pi^2}{a^2} + \frac{2i}{\delta^2} - \frac{4\pi^2}{\lambda^2} = G + EMI - WP \quad (8)$$

where gamma is the complex wavenumber including all three processes, and the symbols G, EMI and WP stand for the geometrical sounding, EM induction and wave propagation term, respectively. The process corresponding to the largest term will dominate, and the other terms may be negligible, depending on their magnitude.

- 20 Since there are four parameters controlling Eq.(6)-(8), which also depend on each other (i.e. permittivity depends on frequency), it is difficult to give an operating range of general validity. It seems more feasible to evaluate the terms in Eq.(8) for specific conditions. For the measurements discussed in this paper, we can carry out the following estimates: The maximum frequency of our system is 240kHz. Assuming a minimum relative permittivity of 3, the minimum wavelength of wave propagation given by Eq.(7) is 722m. The minimum wavelength of EMI given by Eq. (6) depends on electrical resistivity. Assuming $\rho = 100\Omega m$
- 25 as the minimum resistivity, which is a little smaller than the minimum values actually encountered, we obtain approx. 10m for the minimum EMI wavelength. From Eq.(8), it is clear that the geometrical sounding term will be minimum for the largest electrode spacing, and therefore we use our largest spacing $a = 1.5m$ in Eq.(8) to obtain a worst-case estimate.

- With these numbers for the wave lengths, we obtain for the magnitudes: $G = 17.5$; $EMI = 0.02$; $WP = 7.6 \cdot 10^{-5}$. Therefore, the wave propagation term is by far the smallest and can safely be neglected, the EMI term is still significantly smaller than
- 30 the geometrical sounding term. We therefore assume that for the data discussed here, EMI is also negligible, in case of high resistive environments and small electrode distances (Fiandaca, 2018). ~~Thereby, the~~ Nevertheless, we are also aware that a comprehensive assessment requires precise modelling of the equations, which will be subject of future work. If we chose a

larger electrode spacing, $a = 30$ m, then $EMI = 8$, this would be in the same order of magnitude as G , and we would have to carry out a more thorough analysis.

In addition to these purely physical considerations, we also have to take technical issues into account, such as coupling of the capacitive electrodes, and electromagnetic coupling between cables and the ground, which are less simple to estimate or to correct for. Therefore, we consider it necessary to gain experience and to test the entire system under a variety of conditions.

3.3 Single Site Inversion

The single site inversion was the primary method used in Przyklenk et al. (2016). In this spectral approach, the data of each measured 4-point array is inverted separately, i.e. without influence of other measurements. Under the conditions of geometrical sounding, the penetration depth of the measurements measurement is only controlled by the geometric size of the configuration, i.e. the geometry factor K , in contrast to the frequency sounding where the frequency dependent skin depth describes the penetration depth (McNeill, 1980).

The fit of the measured spectral data of the magnitude $|Z(f)|$ and phase shift $\varphi(f)$ is done under parametrisation of the complex impedance (Eq. (2)) by the single Cole-Cole Equation (Eq. (5)). The inversion is based on the model of a homogeneous halfspace. From the result of the inversion, the five Cole-Cole Model parameters can be extracted. Moreover, the single site inversion has the possibility to take the sensor height effects into account. By using the mean electrode height h as an additional free inversion parameter, it is possible to include the effect of electrode height and at the same time determine its value. Thereby, capacitively coupled measurements taken under conditions of strong height influence, in particular on low resistive subsurfaces, can also be evaluated. If the height is neglected during inversion, this can in principle lead to a distortion of the data and erroneous results. Since in the next step we use a conventional 2-D inversion code for spectral IP data, where the height effect is not included into the forward modelling, it is essential to test whether it is justified to neglect it. For this purpose, we carry out the single site inversion twice: first including the height effect by setting the height as a free parameter and once under the assumption of no sensor height, i.e. by fixing it to zero.

Figure 4 shows a representative example of the spectra for magnitude (a) and phase shift (b) from a measurement at profile B-SCH. The points indicate the measured data, the lines are the calculated spectra for the best-fit model. Inversion is done with (CCM h_{inv}) and without (CCM h_0) determination of height. The calculated height for CCM h_{inv} is $7 \cdot 10^{-7}$ m. This is so close to zero that the results exhibit no visible difference in the measured frequency range. The parameters of the Cole-Cole Model, given in the caption of the Figure, have no difference if rounded to a maximum of two decimal places.

The magnitude adopts a value of around $2 \cdot 10^5 \Omega$ for low frequencies, where the curves converge to a constant value. The phase shift covers almost the entire range that is theoretically possible (0 to -90°). The values close to zero for low frequencies indicate a domination of conduction currents, whereas the deviation from zero for increasing frequencies indicates the increasing relevance of displacement currents. It is expected that for higher frequencies out of the measured range, the phase shift approaches the limit of -90° where displacement currents dominate. The aim of measuring the intermediate range with the transition between both current mechanisms has been achieved in this case. The measured spectral signals in Fig. 4 are typical of the whole measurements on the profile. The values of magnitude are decreasing for larger configurations because of

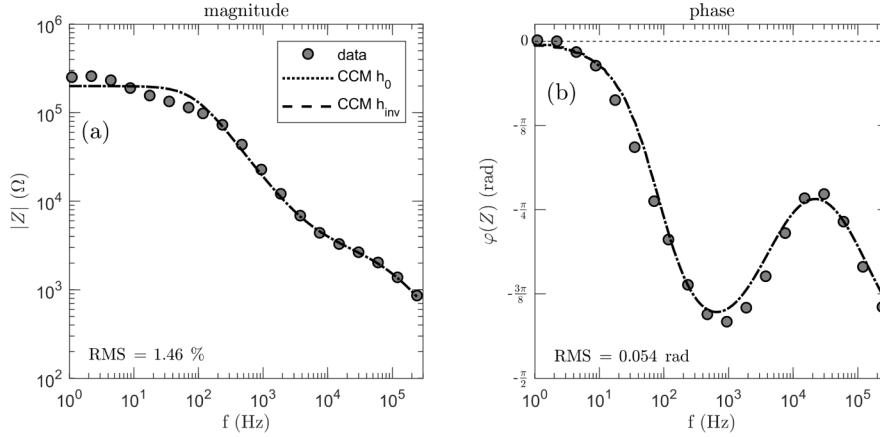


Figure 4. Spectra for the magnitude (a, left) and the phase shift (b, right) of the impedance for measured data (dots) and inversion results by using the Cole-Cole Model (CCM, lines). The inversion was carried out twice, with the assumption of zero electrode height (h_0) and by calculating the height as an additional inversion parameter (h_{inv}). The simulated curves of the two inversions can not be distinguished from each other. Data were measured at profile B-SCH, Schilthorn area, Switzerland, in a dipole-dipole configuration ($a = 1\text{m}$, $n = 1$). The CCM parameters are (h_0 and h_{inv}): $\rho_{DC} = 3.8 \cdot 10^6 \Omega\text{m}$, $\varepsilon_{DC} = 53$, $\varepsilon_{HF} = 2.8$, $\tau = 3.6 \cdot 10^{-5}\text{s}$, $c = 0.82$.

the increasing geometry factor. The phase shift shows the characteristic wavelike shape with a local minimum and maximum. The data fit of the single site inversion is reasonable, justifying the usage of the single Cole-Cole Model.

In case of Lake Prestvannet we assume a sub-vertical separation through the measurements over the lake shore. Two representative signals are shown in Fig. 5 to illustrate the difference between the characteristic curve shapes. The magnitude exhibits a stronger frequency dependence in case of the land measurements and a higher value for low frequencies of about one order compared to the lake measurements. For the phase shift, the shape of the curve measured on the lake is flatter and the local minimum is at higher frequencies. The phase shift shows smaller dynamics for the lake than for the land measurements. The Figure illustrates that the different ground materials provide significant differences in their response.

The inversion was done with and without including the determination of sensor height. For the onshore measurement the estimated height is $2.5 \cdot 10^{-5}\text{m}$, which results in no visible difference between the simulated curves. For the lake measurement the fitted height of $1.2 \cdot 10^{-3}\text{m}$ leads to a visible difference for the phase shift (panel b). The two calculated spectra vary for the lowest frequencies. While the inversion with zero height (continuous line) converges towards zero, the version including height (dashed line) shows a deviation from zero consistent with the data. The data fit shows a difference also in terms of the root mean square (RMS) which is better for CCM h_{inv} . It is known from theory that the height dependence has stronger effects for lower frequencies and is stronger for the phase than for the magnitude of the impedance (Przyklenk et al., 2016). Our data,

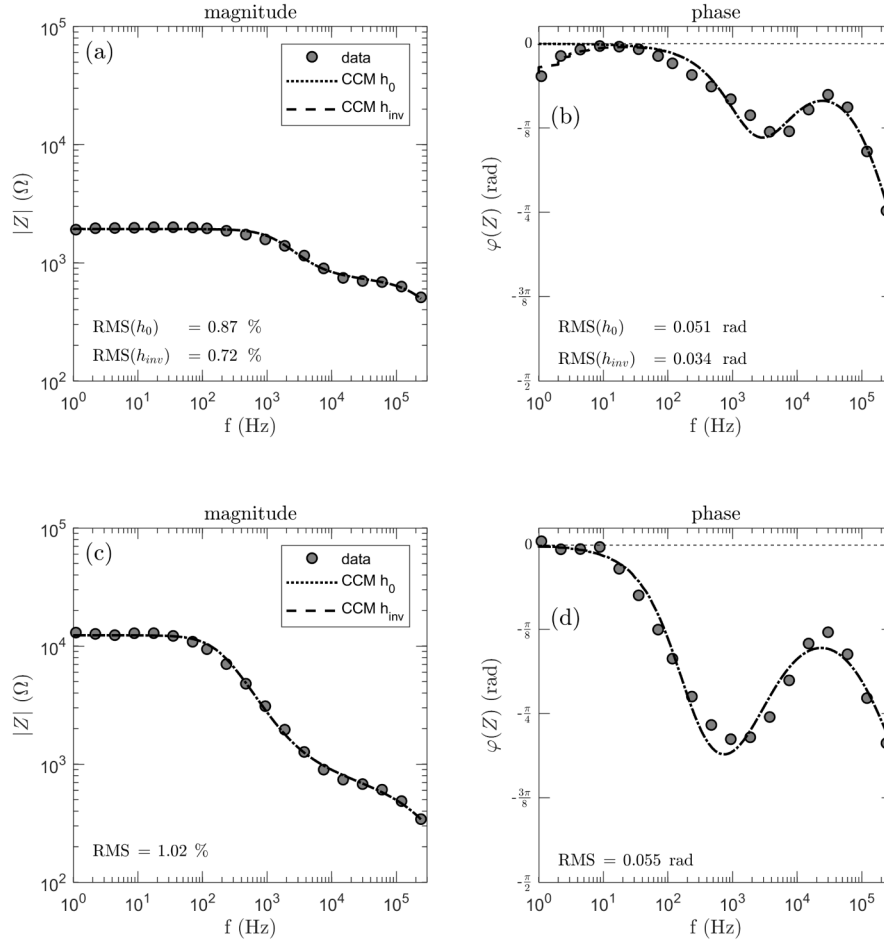


Figure 5. Spectra of two measurements from the Tromsø site. Panel (a,b) show data from the lake and panel (c,d) data from a measurement on shore. The figure shows the measured data and the inversion results using the Cole-Cole Model. The simulated curves with zero electrode height (h_0) and inverted height (h_{inv}) can not be distinguished, except for the phase shift of the lake measurement (panel b). Both measurements were taken with a Wenner-configuration with $a = 1.5$ m.

The CCM parameters for the lake measurement are (h_0/h_{inv}): $\rho_{DC} = 1.82 \cdot 10^4 / 1.81 \cdot 10^4 \Omega\text{m}$, $\varepsilon_{DC} = 374/370$, $\varepsilon_{HF} = 8.80/8.83$, $\tau = 4.2 \cdot 10^{-5} / 4.1 \cdot 10^{-5} \text{s}$, $c = 0.93/0.93$.

The CCM parameters for the onshore measurement are (h_0 and h_{inv}): $\rho_{DC} = 1.2 \cdot 10^5 \Omega\text{m}$, $\varepsilon_{DC} = 670$, $\varepsilon_{HF} = 12.8$, $\tau = 7.1 \cdot 10^{-5} \text{s}$, $c = 0.84$.

with a visible effect in the phase shift and negligible effect in the magnitude for the data set with the smaller impedance (panel a,b) is consistent with these theoretical results.

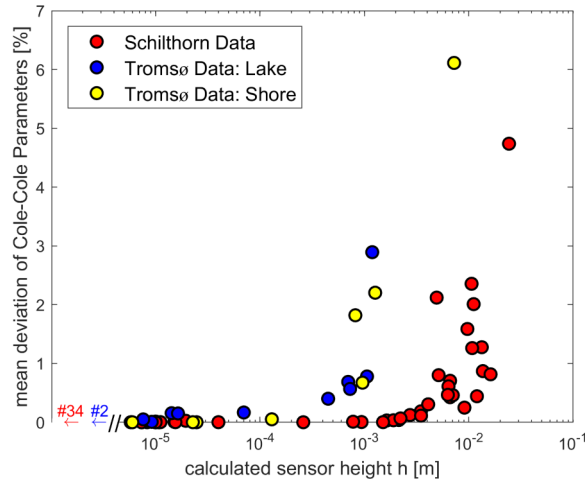


Figure 6. Mean deviation of Cole-Cole parameters vs. sensor height. The deviation was calculated by performing the single site inversion with and without the determination of sensor height and calculating the ratio for all the five Cole-Cole parameters. The data are separately shown for all measurements at profile B-SCH (Schilthorn, red) and for Lake Prestvannet (Tromsø, on the lake (blue) and on shore (yellow)). Values for sensor heights lower than $5 \cdot 10^{-6} \text{ m}$ and $5 \cdot 10^{-6} \text{ m}$ are not displayed but their number of measurements is shown.

3.4 Influence of Electrode Height on Cole-Cole Parameters

In the following, we analyse the dependence of the Cole-Cole parameters on the electrode height in some more detail. The reason is, that the 2-D inversion used later is not able to consider non-zero electrode height. Therefore, the single site inversion was performed for every measured array of both field areas in both versions, with and without determining h . For every array, the five resulting Cole-Cole parameters were put into relation for both inversions and the mean deviation in percent was calculated. This deviation is shown in dependence on the estimated sensor height in Fig. 6.

For larger sensor height, the Cole-Cole results are more affected. The Schilthorn data (red dots) show a strong increase of deviations from approximately $5 \cdot 10^{-3} \text{ m}$ height on, where for. For the Tromsø data, which are shown separately for the measurements on the lake (blue dots) and on shore (yellow dots), this increase occurs for sensor heights about one order of magnitude lower. The different behaviour can be explained by the condition of lower electrical resistivities for the Tromsø measurements. As mentioned earlier, the height effect is stronger for lower ground parameters of resistivity and permittivity. Furthermore, for the Schilthorn data higher values of sensor height were determined. This could indicate that in case of the solid ice surface, as on the lake, the contact of electrodes to the ground is very smooth, resulting in a more homogeneous sensor height. On the other hand, the snow surface at Schilthorn builds a more porous ground. The loose material might cause a poorly defined contact and lead to an artificially increased apparent electrode height. The Schilthorn data shows scattered sensor heights, which indicates the uncertainty in the electrode contact surface. It should be noted that the calculated sensor height in Fig. 6 are shown only down to the lowest values of $5 \cdot 10^{-6} \text{ m}$, but also lower values were determined. Investigations

from Przyklenk et al. (2016) and Kuras et al. (2006) indicate that electrode heights lower than around 10^{-4} m do not effect the measured signal, especially under high resistive conditions. Smaller heights determined by the inversion are mainly caused by numerical reasons and does not represent physical conditions. They can be seen as equal to zero. The determined values of the Schilthorn measurements range from less than 10^{-9} m up to centimeters. On the other hand the Tromsø results only vary from
5 10^{-7} m to the millimeter range.

Additional investigations, which will not be further elaborated here, have indicated that the parameters ρ , ε_{DC} and τ are generally more affected than ε_{HF} and c . That is consistent to the fact that the electrode height effects mainly the lower frequencies. All in all, the deviations of the Cole-Cole results are relatively small. Except for the two highest values in Fig. 6, their effect is smaller 3 percent. These deviations are considered to be acceptable, compared to the typical Cole-Cole parameter
10 resolution for inversions (Yuval and Oldenburg, 1997; Madsen et al., 2017). The results justify therefore the use of inversions without considering effective sensor height, as in the case of the 2-D inversion (see next section). It should be noted that under less favourable conditions, depending on the electrical parameters of the soil and the texture of the surface, neglecting the height can lead to larger errors. Neglecting height is therefore not a general recommendation, but has to be investigated separately for each application with different subsurface conditions. In the case of snow or icy ground, one additional benefit
15 is that these are rather smooth surfaces, where the electrode height is small. On uneven surfaces, such as gravel and rock fields, an installation of the plate electrodes without height variations may be difficult to achieve.

4 2-D Inversion with AarhusInv

The full spectral inversion of complex resistivity data, where all frequencies are being inverted simultaneously, has been a challenge for some time. For example, Grimm and Stillman (2015) used a workaround based on the time-lapse feature of
20 RES2DINV (Loke and Barker, 1996) to invert their broadband SIP data from a periglacial environment. Recently, a few codes for full spectral inversion have become available (Günther and Martin, 2016; Maurya et al., 2018). Here, we use the program AarhusInv (as in Maurya et al. (2018))(as in Maurya et al., 2018), which is a tool for the inversion and modelling of geophysical data for several measurement methods (Auken et al., 2014). The software is freely available for non-commercial purposes.
25 In AarhusInv the complex impedance is modelled in 2-D solving the Poisson's equation, Fourier transformed in the strike direction, without considering EM effects (Fiandaca et al., 2013). All the inversion parameters are inverted simultaneously using all the measured frequencies in a unique inversion process (equivalently to the spectral full-decay inversion of the time-domain IP data). In case of Induced Polarization, where the frequency range is usually only up to one kilohertz, in general relatively small phase shifts are measured. In order to use the inversion for the CCR method, we included the permittivity Cole-Cole Model defined by Eq. (5) to parameterize the frequency-dependent electrical properties. Compared to the conventional Cole-Cole
30 resistivity model that is defined by four parameters and is sometimes used to parameterize low-frequency SIP spectra (Pelton et al., 1978; Tarasov and Titov, 2013), the model defined by Eq. (5) has one more parameter, basically corresponding to the high-frequency limit of permittivity. Therefore, the result of the inversion is a distribution of the five Cole-Cole parameters. As discussed previously, the height of the electrodes is not included into AarhusInv and assumed to be zero. Through this approx-

imation the application for CCR data is usually just suitable under highly resistive conditions. Of course, this inversion method could generally be used for high frequency spectral resistivity measurements, including galvanically coupled electrodes.

In the following, we will show the results of the 2-D inversion for both field sites. The resulting distribution of all Cole-Cole parameters will be discussed and compared with the expected properties of the subsurface.

5 4.1 Schilthorn

The measured data from profile B-SCH were evaluated by the 2-D inversion. The result is shown in Fig. 7, where several 2-D models for the five Cole-Cole parameters ρ , ε_{DC} , ε_{HF} , τ and c are shown color-coded vs. depth and horizontal coordinate.

The dashed black line corresponds to the manually measured depth of the top snow layer. ~~The brighter areas are those below a~~

~~In this context, it is important to discuss the resolution of the Cole-Cole parameters, because it is known from previous~~

10 ~~studies that it can be difficult to reliably estimate relaxation time and frequency exponent (e.g. Madsen et al., 2017). The~~

~~problems usually arise if the frequency where the phase peak occurs, which is related to the relaxation time, is outside the~~

~~measured acquisition range. Weigand and Kemna (2016) discuss similar observations when average parameters are derived~~

~~from spectral decomposition techniques. The particular benefit of our acquisition system is the wide frequency range compared~~

~~to conventional SIP system. As a result, all phase peaks corresponding to the relaxation times are in fact being measured.~~

15 ~~Therefore, we are confident that the Cole-Cole parameters of the inversion results are well determined. Nevertheless, we~~

~~carried out additional experiments where we fixed the frequency exponent c , as suggested by Weigand and Kemna (2016). In~~

~~that case, the data fit deteriorates, in the sense that the curve shape vs. frequency cannot be matched that well any more. We~~

~~consider this as evidence that even c is not poorly constrained. The strong variability of c observed in the inversion results~~

~~may be justified by the actual change in materials. Finally, we rely on the~~ depth of investigation ~~value (DOI) ; areas where the~~

20 ~~parameters can no longer be reliably estimated~~ as an objective measure in which regions parameters are well constrained. The

calculation of the DOI was described in Fiandaca et al. (2015). ~~The brighter areas in Fig. 7 are those below the DOI, areas~~

~~where the parameters can no longer be reliably estimated.~~ This boundary differs for each parameter, having in most cases the

deepest extent for the resistivity model. ~~This suggests that resistivity is better constrained than the other parameters. It should~~

~~be noted that the measurements were not carried out with the same electrode spacing throughout the profile. Measurements~~

25 ~~with wider electrode spacing and corresponding larger penetration depth were carried out only on the first half of the profile.~~ We

~~are aware that other tools to assess parameter resolution may exist, but a comprehensive treatment of this subject is beyond the~~

~~scope of this paper.~~

First, we focus on the structural aspects of the results. The structure is a little different for each of the five sections, but in general a structure of two layers can be recognized, representing the top snow layer and the underlying surface layer. Because

30 of the additional snow depth measurements, the results of the inversion can be validated. Especially for ε_{DC} , the boundary of

the snow layer agrees well with the corresponding parameter contrasts. Around profile meter 20, where the boundary indicates

a ditch, it becomes particularly clear how precisely the layer structure is reflected by the low-frequency permittivity value

(panel b). The layer boundary can also be seen from the result of the resistivity (panel a), where a highly resistive surface layer

is followed by a more conductive material. Unlike in the ε_{DC} section, there is a continuous decrease in the value with the

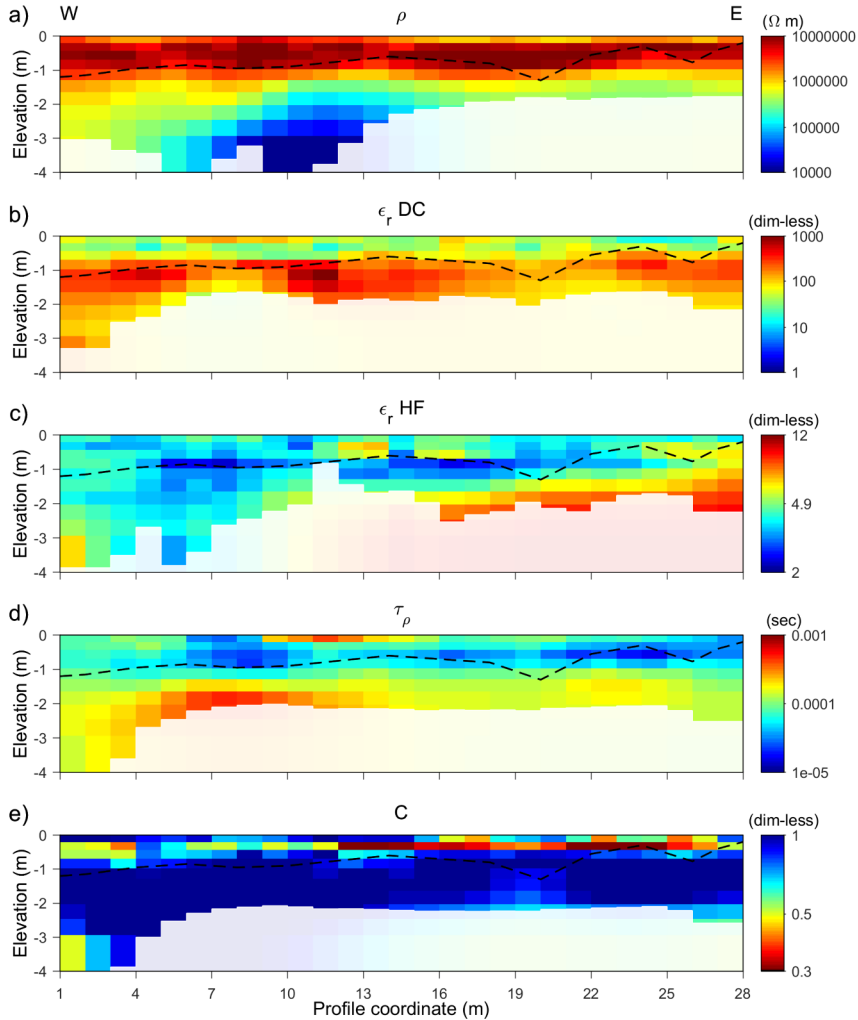


Figure 7. Result of the AarhusInv 2-D inversion for the data from the Schilthorn area along the profile B-SCH denoted in Fig. 1. The figure shows the sections of the five Cole-Cole parameters (a-e) defined by eq. (5). The dashed line shows the separately measured depth of the snow-layer, the brighter parts represents the area where the depth of investigation is exceeded.

depth, which makes the layer transition appear more smoothly. The layer boundary is also apparent in the section of parameter τ (panel d). The relaxation exponent c (panel e) also indicates the boundary. In the lower layer, c is close to 1, corresponding to a Debye relaxation. Compared to the other parameters, less literature is available for the relaxation exponent and the values are close to each other. Therefore, c seems less suitable for an interpretation in terms of material properties. The high frequency value ε_{HF} (panel c) is the only one which does not show a clear distribution. The range in this case is significantly smaller compared to the other parameters, which could make it more difficult to identify differences in materials based on ε_{HF} . This is the case in this example but could be different for other test sites or under different condition. The region of slightly higher

values at about two meter depth on the second half of the profile could indicate a systematic change in the permittivity.

The two layers could be identified as the snow layer and the underlying bedrock, expected as limestone layer described by Rowan (1993), which could also be seen at some spots on the surface near the profile area. The resistivity and the relaxation time on the first half of the profile show some more variation underneath the snow; ~~possibly~~. This could be caused by a

5 ~~third layer of weathered material on top of the bedrock~~. ~~It is unclear whether the layer of limestone or possible weathered material under the snow is frozen or unfrozen. For the time of measurements the subsurface is usually unfrozen, but as the snow cover isolates the ground, the subsurface could be slightly frozen or a possible ice cover underneath the snow, as described by Scherler et al. (2010).~~

The determined values in their dominating range for the two horizontal regions of profile B-SCH are compared to literature in
10 table 1. The literature values of the different materials can vary over large ranges, which is mainly caused by the differences in physical conditions. For ice and snow the purity, density, salinity and temperature can strongly influence the electrical parameters (~~Arenson et al., 2015; Evans, 1965~~) (Auty and Cole, 1952; Arenson et al., 2015; Evans, 1965). New and soft snow, as it was present in case of the Profile B-SCH, has a relatively low density, meaning an increase of resistivity towards more dense snow. For the literature values of ice the attribute pure means that there is no impurity caused by other materials in the
15 ice/water, but there are still variations based on the physical conditions like temperature. If ground material is frozen, like on permafrost or seasonal frost, the measured signal is expected to react as a composition of the basic material and ice (Zorin and Ageev, 2017). The parameters for frozen ground are strongly dependent on the ice content and temperature (Arenson et al., 2015; Grimm et al., 2015). In the case of limestone, laboratory investigations of CCR by Murton et al. (2016) showed, that the resistivity of a frozen limestone sample ($10^5 \Omega m$) can be one order of magnitude higher than for the same sample in an
20 unfrozen state.

The electrical behaviour of water needs particular attention, because the typical relaxation frequency of water is in the range of GHz (e.g. Artemov and Volkov, 2014). Consequently, the high frequency value ϵ_{HF} of about 5 will not be reached within our frequency range. Instead, the real dielectric permittivity exhibits a constant behaviour, denoted as the low frequency value, which is commonly known as 80. However, a study by Seshadri et al. (2008) shows, that even in water without solids another relaxation process takes place at lower frequencies in the range of Hz, associated with interfacial polarization due to ions. The dielectric permittivity therefore can reach values of more than 1000 at the lower boundary of our frequency range, especially if the water has a high electrolyte concentration.

In ~~summary, the determined~~ table 1 (top row) the information of the inversion results (Fig. 7) is extracted and attributed to different layers. For the first layer, the estimated values agree for all Cole-Cole parameters from the 2-D inversion are consistent with the literature values for the expected materials. The parameters of the top layer correspond to the values parameters with those of snow. For the ~~underlying layer, the literature for limestone~~ area under the horizontal boundary, indicated by the clear change in parameters ρ_{DC} , ϵ_{DC} and τ , the estimated values are in agreement with the estimated values. The further separation in resistivity could expected limestone layer. As the resistivity indicates a further separation, the area directly underneath the snow could either belong to an ice layer or be caused by a frozen state, ~~which should increase the value of pure limestone, or could be caused by general differences in material.~~ followed by a less resistive part of the limestone. The observation that all other

Table 1. Results of the 2-D inversions on profile B-SCH and the profile on Lake Prestvannet and comparison with literature values for snow, ice, water and limestone, which is expected as bedrock material on B-SCH. The characteristic parameters from the inversions are given as the range for the two horizontal layers for profile B-SCH and the two vertical separated regions of lake and shore for the profile on the Lake Prestvannet. Literature values were taken from Arenson et al. (2015)¹, Evans (1965)², Achammer and Denoth (1994)³, Palacky (1988)⁴, Murton et al. (2016)⁵, Olatinsu et al. (2013)⁶ and, Seshadri et al. (2008)⁷, [Artemov and Volkov \(2014\)](#)⁸ and [Auty and Cole \(1952\)](#)⁹.

		$\rho_{DC} [\Omega m]$	$\varepsilon_{DC} [-]$	$\varepsilon_{HF} [-]$	$\tau [s]$
B-SCH	First Layer	$10^6 - 10^7$	15 - 100	2 - 9	$10^{-5} - 10^{-4}$
	Second Layer	$10^3 - 10^6$	50 - 700		$10^{-4} - 5 \cdot 10^{-4}$
Lake Prestvannet	Lake	$10^4 - 2 \cdot 10^4$	750 - 3000	5 - 11	$10^{-4} - 6 \cdot 10^{-4}$
	Shore	$4 \cdot 10^5 - 10^4$	850 - 6500	12 - 15	$6 \cdot 10^{-5} - 2 \cdot 10^{-4}$
Literature	Snow ^{1,2,3}	$10^5 - 10^8$	~ 40	< 15	$\sim 10^{-4}$
	Limestone (unfrozen/frozen) ^{4,5,6}	$10^3 - 10^5$	50 - 130	5 - 9	$2 \cdot 10^{-5} - > 10^{-4}$
	Ice (pure) ^{2,7,2,7,8,9}	$10^5 - 10^9$	92 - 105	3	10^{-4} $2.2 \cdot 10^{-5} - 5 \cdot 10^{-3}$
	Water ^{2,7,8}	$< 10^6$	<u>80</u>	<u>5 (> GHz)</u>	<u>$10^{-12} - 10^{-10}$</u>

[parameters except resistivity show no significant change in this area can be explained by the similarity of the parameters for ice and limestone, indicated by the literature values. The similarity and small range of high frequency permittivity \$\varepsilon_{HF}\$ of all corresponding literature values can explain the low variability and missing distinctness in this parameter section. In summary, the determined Cole-Cole parameters from the 2-D inversion are consistent with the literature values for the expected materials.](#)

- 5 A comparison with the results of the single site inversion illustrates the differences of the inversion methods. Figure 8 shows the results for the same measurements as in Fig. 7 but evaluated by the single site inversion. The parameters are determined individually for each quadrupolar measurement. In order to represent the results in a two-dimensional structure, the **results parameters** are assigned to a certain location according to the midpoint position and extent of the array. Thus, a two-dimensional pseudo-section is finally created for each parameter, which can provide a rough overview of the subsurface structure. **One has**
- 10 **to keep in mind, that the pseudo-sections in** [The difference between Fig. 7 and Fig. 8 is that Fig. 8 show inverted data and not just measured data as it is for example in the case of DC resistivity measurements](#) [represents an inversion result only with respect to frequency, but a pseudo-section with respect to the spatial distribution, where as Fig. 7 is a full inversion result with respect to both frequency and space.](#) As expected when comparing pseudo-sections with 2-D inversion results, overall structures are similar, but there are differences in detail. The low-frequency permittivity (panel b) and the relaxation time (panel
- 15 d) systematically increase with depth, while the resistivity (panel a) shows a decrease with depth, all indicating a horizontally layered structure. As seen before in the 2-D results, the high permittivity value ε_{HF} exhibits a small range of values and does not show a systematic distribution, but fits in the range of the literature. Since the results of the deeper pseudo-layers always represent an integral value over the entire depth range, it has to be expected that clear boundaries between the layers can not be identified by this method. Therefore the measurements have to be analysed in dependence to each other, as it was done by the

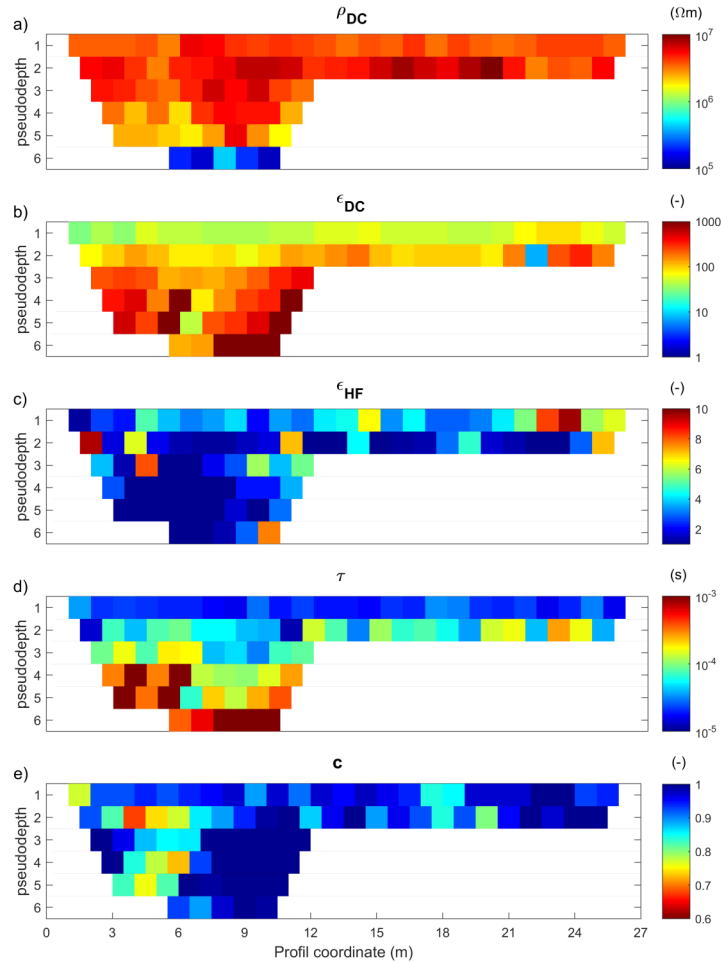


Figure 8. Pseudosections of the five Cole-Cole parameters (a-e) calculated by the single site inversion for profile B-SCH. Measurements were done for larger configurations on the left half of the profile.

2-D inversion. However, since the inversion with respect to the frequency dependence is independent for the two methods, we take the qualitative consistency as evidence that our 2-D inversion is a feasible tool to invert spatial and frequency dependence at the same time.

4.2 Tromsø

- 5 The investigations at Lake Prestvannet focus on the vertical transition from the lake to the shore rather than on the distribution with depth. In Fig. 9, the result of the AarhusInv 2-D inversion is shown for all Cole-Cole parameters. Measurements were

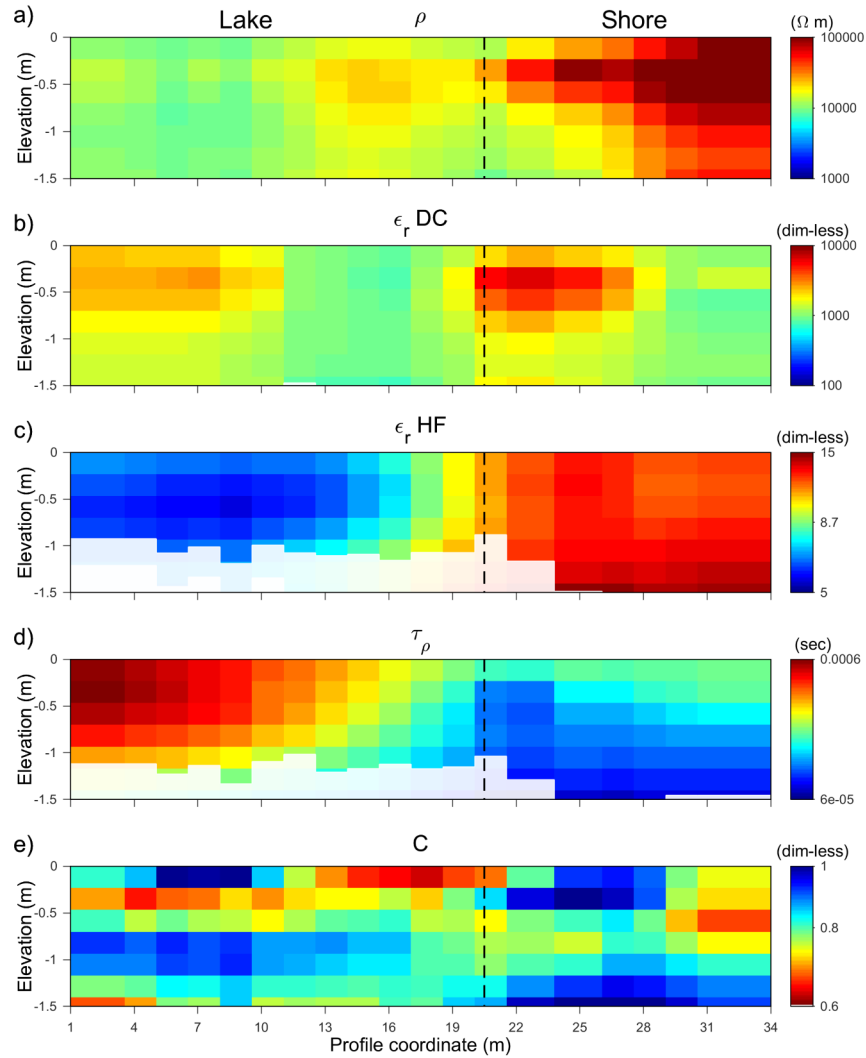


Figure 9. 2-D inversion result of the 5 Cole-Cole parameters (a-e) for the measurements at the lake Prestvannet denoted in Fig. 3. The surface boundary between lake and shore is at profile meter 20.5, indicated by the dashed line, where a change in most parameters can be recognized. The whitened areas are those where the value of DOI is exceeded.

carried out for just a small spacing (Wenner $a = 1.5$ m), so the penetration depth is not more than approximately 1.5 meters. Brighter areas are again below the DOI and the vertical black line indicates the surface position of the transition from the lake to the shore at profile meter 20.5. Except for the relaxation exponent c (panel e), in all models the transition is defined by a parameter change. The ranges of the estimated Cole-Cole parameters for lake and shore are given in table 1 and can be

5 compared to the literature values of [snow and ice](#), [ice and water](#).

The high-frequency permittivity ε_{HF} (panel c) shows lower values for the lake than onshore. This parameter is somewhat specific, because the variation from lake to shore is the only prominent variation, whereas the other parameters also show some structure within both sides. Compared to profile B-SCH (Fig. 7), where ε_{HF} has a small dynamic range with little spatial coherence, for the data of Lake Prestvannet both permittivity values ε_{DC} and ε_{HF} seem to be useful to distinguish different materials or the state of freezing. The low-frequency permittivity ε_{DC} (panel b) shows the transition from lake to shore, but exhibits additional variation on either side of the transition. The land side shows an anomaly close to the transition. The cause is not exactly known, but we hypothesize that it indicates a change in sediments. A detailed analysis, where the two properties of permittivity may be combined with resistivity in a multi-parameter analysis may be a subject of future research. The relaxation time τ shows relatively homogeneous values for each of the sides. The fact, that the relaxation times of snow are shorter than those of ice (Evans, 1965) is consistent with our results. The resistivity ρ_{DC} decreases from higher values on the snow covered land side, by about one order of magnitude on the lake. The relaxation exponent c shows small variations and poor spatial coherence, and is difficult to interpret in terms of material variations.

Onshore, the measurements were taken on the snow and the known values of snow are consistent for some parameters. Higher density of the snow could explain the much lower resistivity than obtained for the snow at B-SCH. However, in combination with the values of ε_{DC} which are higher than expected for snow, this could indicate that the measurements are under the influence of the ground material beneath. For the frozen lake, the values estimated from the inversion are a bit higher than typical literature values for ice. However, it is known that the electrical parameters of frozen water bodies can be very different from those of pure ice. The lake ice could be a composition of ice and partly water, ~~insteat~~ instead of a pure ice body. Such mixtures can result in ~~much~~ higher values of permittivity, ~~because water has a value ε_{HF} of~~. The high salinity of the lake can further increase the low frequency permittivity of the water to the range of > 1000 (Seshadri et al., 2008). This is significantly larger than the value of pure water of about 80 (Evans, 1965), and could explain the high ε_{DC} values determined by the inversion. At the high-frequency end in our frequency range, the value of ε_{HF} is probably also controlled by water (around 80 in that frequency range), which explains why our estimated value is larger than that expected for pure ice. Lower values of resistivity could as well be explained by this composition because water has a lower intrinsic resistivity than ice. A similar observation was made by Przyklenk et al. (2016) during their discussion of measurements on mountain ice.

4.3 Data fit

For the assessment of the inversion results, we consider their quality in terms of the data fit. Because of being a spectral inversion, the inversion includes the fit of all measured data over frequency, corresponding to a spectral pair of magnitude and phase shift for every 4-point-array. In the following, the data misfit is expressed in terms of the weighted mean square error, where each difference is weighted by the inverse of the data error. This value is denoted by the symbol χ , and is a well established measure of the misfit. Together with an additive regularization term, it is minimized during the inversion (Fiandaca et al., 2013).

Figure 10 shows the data fit for the 2-D inversion of the Schilthorn measurements. The top panel (a) shows the misfit of amplitude and phase shift over the profile length. The residuals are averaged over all measurements with all configurations

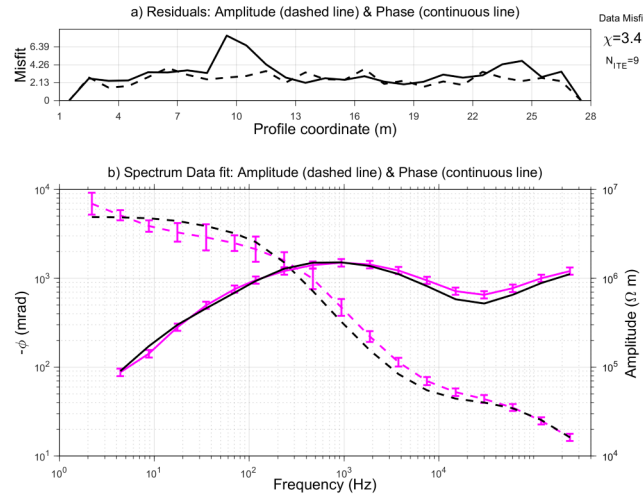


Figure 10. Data fit of the 2-D inversion of profile B-SCH. The top panel shows the misfit of amplitude (blue dashed line) and phase shift (red solid line) over the profile. The bottom panel shows an example of measured (red) and inverted (black) spectra of amplitude (dashed lines) and phase (continuous lines), which belong to the dipole-dipole measurement starting from profile meter 16 ($a = 1$ m, $n = 1$) along the profile direction (see fig. 7). The measured data is the same as in figure 4, with resistivity instead of impedance, and phase shift on a logarithmic scale. The total data misfit is $\chi = 3.4$ after 9 iterations. For each profile coordinate, the misfit of all data corresponding to this point were averaged to obtain the top panel.

with the same midpoint. The total inversion misfit is $\chi = 3.4$, based on the average relative standard deviation of amplitude (0.16) and phase measurements (0.10). The inversion converged after nine iterations. The misfits of amplitude and phase are homogeneous over the profile, except around profile meter 10, where the phase misfit is significantly higher. As can be seen from Fig. 7, this is the area where ρ and τ show another change for the deeper region. The higher misfit corresponds to the data of larger configurations (dipole-dipole with $n = 5, 6$), where the measured signals show slightly different curves than for the shallower measurements. The large misfit indicates that the deep structure should be treated with caution because it could be caused by difficulties in matching data.

Panel (b) of Fig. 10 shows the data fit of the spectrum, which was previously shown during the discussion of the single site inversion (Fig. 4). Data and inversion results are shown for the amplitude (dashed lines) and the phase (continuous lines). The amplitude is not exactly the same as the magnitude in Fig. 4, but was converted to the frequency dependent resistivity (using Eq. (3)). The negative phase shift is displayed on a logarithmic scale in *mrad*. Some data points, in this case for the two lowest frequencies, that caused difficulties for the inversion code and were identified as outliers, are not shown. Overall, for both amplitude and phase shift, the shape of the spectrum is well matched. For several data points, the calculated curve is not within the data errors, which is reflected in a misfit value $\chi > 1$. The data errors are calculated by the device by stacking multiple measurements. Considering that broadband electrical data of 79 spectra were matched with a single 2-D model, we find the fit satisfactory. The 19 discrete measured frequencies seem to be sufficient to define the dispersion of permittivity.

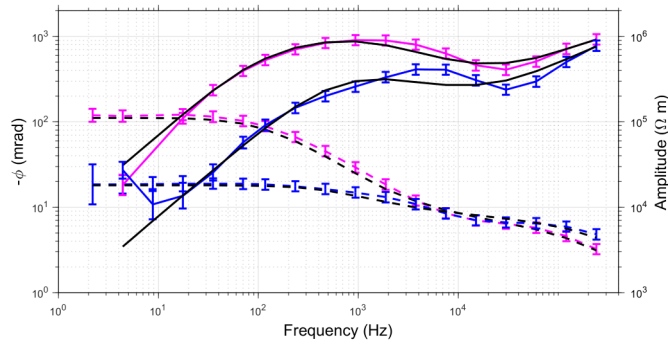


Figure 11. Data fit of the 2-D inversion for two stations of the lake Prestvannet profile. The blue lines correspond to a [station measurement](#) at 11.5 m, which is on the lake, the red [line lines](#) to [a station an onshore measurement](#) at 28 m, [onshore with the corresponding inverted spectra](#) (black). Both were measured with a Wenner configuration ($a = 1.5$ m). The measured data are the same as in figure 5. The amplitude is indicated by the dashed lines and the phase shift by the solid lines.

Another example of data spectra is shown in Fig. 11 for the measurements taken at Lake Prestvannet. The data are the same as discussed in Fig. 5, with one lake measurement (blue) and one onshore measurement (red) corresponding to profile coordinates 11.5 m and 28 m from Fig. 9. The total data misfit of the inversion is $\chi = 1.8$. The onshore spectra shows some similarity to the Schilthorn spectra (Fig. 10). The amplitude and the phase shift are both matched very well. As mentioned before for the single site inversion, the spectra of lake and land show a different frequency-dependent behaviour. A slight difference between the measured and calculated data is visible for the phase of the lake measurement in the intermediate frequency range. This could indicate limitations of the single Cole-Cole model.

The sensor height effect is not negligible in this case. The lowest two frequencies seem to be affected and can not be matched by the inversion. This is the same effect as discussed previously during the single site inversion.

10 5 Conclusions

Wide-band complex resistivity measurements based on capacitively coupled electrodes were carried out on two cryospheric field sites, on a frozen lake in Norway and in an alpine region in Switzerland. By recording the spectral data in an intermediate frequency range, where conduction currents and displacement mechanisms are relevant, the determination of the frequency-dependent electrical resistivity and permittivity is investigated. The data analysis is done by a novel 2-D inversion for broad-band electrical measurements based on the inversion tool AarhusInv, where the permittivity is parameterized with a Cole-Cole model.

The first applications of the 2-D inversion give encouraging results in the sense of consistence with known materials and structure. For our shallow field measurements, the single Cole-Cole model seems sufficient and there is no evidence of fundamental difficulties in fitting spectral data. The observed misfits are acceptable in a sense that χ is close to 1, in the range typical for

conventional 2-D resistivity inversions, and should have similar causes, such as 3-D effects. In principle, it is possible to implement a double Cole-Cole model, which could fit more complex spectra, but has more inversion parameters. The assumption of zero sensor height seems to be uncritical in our chosen field applications. In some cases, it could be helpful to discard some low-frequency data, which are most strongly affected by electrode height above the observed surface.

- 5 The determination of the electrical parameters ~~was successful and they are reasonably consistent for both investigations was successful. They show reasonable consistence~~ with literature values within a maximum deviation of one order of magnitude. The inversion for the five Cole-Cole parameters works as well as conventional 2-D resistivity inversion, except for the frequency exponent, which tends to show spatially incoherent images. The complementary information provided by the high- and low-frequency limits of permittivity can be significant. Some structures are more clearly defined than in the corresponding
- 10 resistivity image. We conclude that using different parameter sections for the interpretation can lead to a more differentiated analysis of the subsurface.

The full spectral information can be used for the determination of ground ice content at the field scale, as suggested by Grimm and Stillman (2015). This is an objective of research in periglacial environments, and will be a subject of future work.

- Acknowledgements.* We are grateful to Katharina Bairlein (PTB, Braunschweig) and Christian Kulüke (TU Braunschweig) for the support
- 15 of our measurements in Norway and Switzerland. We thank Wim Weber (City of Tromsø) for the permission to take the data on the lake Prestvannet.

The work was sponsored by the German Research Foundation (projects HO 1506/22-1 and HO 1506/22-2), and by the University of Aarhus.

References

- Achammer, T. and Denoth, A.: Snow dielectric properties: from DC to microwave X-band, *Ann Glaciol*, 19, 92 – 96, <https://doi.org/10.3189/S0260305500011034>, 1994.
- Arenson, L., Colgan, W., and Marshall, H.: Physical, Thermal, and Mechanical Properties of Snow, Ice, and Permafrost, In: *Snow and Ice-Related Hazards, Risks and Disasters*, <https://doi.org/10.1016/B978-0-12-394849-6.00002-0>, 2015.
- Artemov, V. and Volkov, A.: Water and Ice Dielectric Spectra Scaling at 0°C, *Ferroelectrics*, 466, 158–165, <https://doi.org/https://doi.org/10.1080/00150193.2014.895216>, 2014.
- Auken, E., Christiansen, A., Kirkegaard, C., Fiandaca, G., Schamper, C., Behroozmand, A., Binley, A., Nielsen, E., Effersø, F., Christensen, N., Sørensen, K., Foged, N., and Vignoli, G.: An overview of a highly versatile forward and stable inverse algorithm for airborne, ground-based and borehole electromagnetic and electric data, *Explor Geophys*, 46, 223 – 235, <https://doi.org/10.1071/EG13097>, 2014.
- Auty, R. and Cole, R.: Dielectric Properties of Ice and Solid D₂O, *J Chem Phys* 1309 (1952);, 20, 1309, <https://doi.org/https://doi.org/10.1063/1.1700726>, 1952.
- Bittelli, M., Flury, M., and Roth, K.: Use of dielectric spectroscopy to estimate ice content in frozen porous media, *Water Resour Res*, 40, W04 212, <https://doi.org/10.1029/2003WR002343>, 2004.
- 15 Cole, K. and Cole, R.: Dispersion and Absorption in Dielectrics: 1. Alternating Current Characteristics, *J Chem Phys*, 9, 341 – 351, <https://doi.org/10.1063/1.1750906>, 1941.
- Dashevsky, Y., Dashevsky, O., Filkovsky, M., and Synakh, V.: Capacitance Sounding: a New Geophysical Method for Asphalt Pavement Quality Evaluation, *J Appl Geophys*, 57, 95 – 106, <https://doi.org/10.1016/j.jappgeo.2004.10.001>, 2005.
- Duvillard, P., Revil, A., Qi, Y., Soueid Ahmed, A., Coperey, A., and Ravel, L.: Three-Dimensional Electrical Conductivity and Induced Polarization Tomography of a Rock Glacier, *J Geophys Res-Sol Ea*, 123, 9528 – 9554, <https://doi.org/10.1029/2018JB015965>, 2018.
- 20 Evans, S.: Dielectric Properties of Ice and Snow – a Review, *J Glaciol*, 5, 773 – 792, <https://doi.org/10.3189/S0022143000018840>, 1965.
- Fiandaca, G.: Induction-free acquisition range in spectral time- and frequency-domain induced polarization at field scale, *Geophys J Int*, <https://doi.org/10.1093/gji/ggy409>, 2018.
- Fiandaca, G., Ramm, J., Binley, A., Gazoty, A., Christiansen, A., and Auken, E.: Resolving spectral information from time domain induced polarization data through 2-D inversion, *Geophys J Int*, 192, 631 – 646, <https://doi.org/10.1093/gji/ggs060>, 2013.
- 25 Fiandaca, G., Christiansen, A., and Auken, E.: Depth of Investigation for Multi-parameters Inversions, *European Association of Geoscientists and Engineers. Near Surface Geoscience 2015. Conference Paper*, 631 - 646, <https://doi.org/10.3997/2214-4609.201413797>, 2015.
- Flageul, S., Dabas, M., Thiesson, J., Rejjiba, F., and Tabbagh, A.: First in situ test of a new electrostatic resistivity meter, *Near Surf Geophys*, 11, 265 – 273, <https://doi.org/10.3997/1873-0604.2012063>, 2013.
- 30 Günther, T. and Martin, T.: Spectral two-dimensional inversion of frequency-domain induced polarization data from a mining slag heap, *J Appl Geophys*, 135, 436 – 448, <https://doi.org/10.1016/j.jappgeo.2016.01.008>, 2016.
- Grard, R.: A quadrupolar array for measuring the complex permittivity of the ground: application to Earth prospecting and planetary exploration, *Meas Sci Technol*, 1, 295 – 301, 1990.
- Grard, R. and Tabbagh, A.: A mobile four-electrode array and its application to the electrical survey of planetary grounds at shallow depth, *J Geophys Res*, 96, 4117 – 4123, <https://doi.org/10.1029/90JB02329>, 1991.
- 35 Grimm, R. and Stillman, D.: Field Test of Detection and Characterisation of Subsurface Ice using Broadband Spectral-Induced Polarisation, *Permafrost Periglac*, 26, 28 – 38, <https://doi.org/10.1002/ppp.1833>, 2015.

- Grimm, R., Stillman, D., and MacGregor, J.: Dielectric signatures and evolution of glacier ice, *J Glaciol*, 61, 1159 – 1170, <https://doi.org/10.3189/2015JoG15J113>, 2015.
- Hauck, C. and Kneisel, C.: Application of Capacitively-coupled and DC Electrical Resistivity Imaging for Mountain Permafrost Studies, *Permafrost Periglac*, 17, 169 – 177, <https://doi.org/10.1002/ppp.555>, 2006.
- 5 Hauck, C. and Kneisel, C.: *Applied Geophysics in Periglacial Environments*, Cambridge Univ. Press, <https://doi.org/10.1017/CBO9780511535628>, 2008.
- Hauck, C., Böttcher, M., and Maurer, H.: A new model for estimating subsurface ice content based on combined electrical and seismic data sets, *Cryosphere*, 5, 453 – 468, <https://doi.org/10.5194/tc-5-453-2011>, 2011.
- Hilbich, C., Hauck, C., Hoelzle, M., Scherler, M., Schudel, L., Völksch, I., Vonder Mühll, D., and Mäusbacher, R.: Monitoring mountain
 10 permafrost evolution using electrical resistivity tomography: A 7-year study of seasonal, annual, and long-term variations at Schilthorn, Swiss Alps, *J Geophys Res*, 113, F01S90, <https://doi.org/doi:10.1029/2007JF000799>, 2008.
- Hördt, A., Weidelt, P., and Przyklenk, A.: Contact impedance of grounded and capacitive electrodes, *Geophys J Int*, 193, 187 – 196, <https://doi.org/doi:10.1093/gji/ggs091>, 2013.
- Imhof, M., Pierrehumbert, G., Haeberli, W., and Kienholz, H.: Permafrost Investigation in the Schilthorn Massif, Bernese Alps, Switzerland,
 15 *Permafrost Periglac*, 11, 189 – 206, 2000.
- Kemna, A., Binley, A., Ramirez, A., and Daily, W.: Complex resistivity tomography for environmental applications, *Chem Eng J*, 77, 11 – 18, [https://doi.org/10.1016/S1385-8947\(99\)00135-7](https://doi.org/10.1016/S1385-8947(99)00135-7), 2000.
- Kemna, A., Binley, A., Cassiani, G., Niederleithinger, E., Revil, A., Slater, L., Williams, K., Flores Orozco, A., Haegel, F.-H., Hördt, A.,
 Kruschwitz, S., Leroux, V., Titov, K., and Zimmermann, E.: An overview of the spectral induced polarization method for near-surface
 20 applications, *Near Surf Geophys*, 10, 453 – 468, 2012.
- Kuras, O., Beamish, D., Meldrum, P., and Ogilvy, R.: Fundamentals of the capacitive resistivity technique, *Geophysics*, 71, No.3, 135 – 152, <https://doi.org/doi:10.1190/1.2194892>, 2006.
- Kuras, O., Beamish, D., Meldrum, P., Ogilvy, R., and Lala, D.: Capacitive Resistivity Imaging with Towed Arrays, *J Environ Eng Geoph*,
 12, 267 – 279, <https://doi.org/10.2113/JEEG12.3.267>, 2007.
- 25 Loewer, M., Günther, T., Igel, J., Kruschwitz, S., Martin, T., and Wagner, N.: Ultra-broad-band electrical spectroscopy of soils and sediments—a combined permittivity and conductivity model, *Geophys J Int*, 210, 1360 – 1373, <https://doi.org/Rapid least-squares inversion of apparent resistivity pseudosections by a quasi-Newton method>, 2017.
- Loke, M. and Barker, R.: Rapid least-squares inversion of apparent resistivity pseudosections by a quasi-Newton method, *Geophys Prospect*,
 44, 131 – 152, 1996.
- 30 Madsen, L., Fiandaca, G., Auken, E., and Christiansen, A.: Time-domain induced polarization - an analysis of Cole-Cole parameter resolution and correlation using Markov Chain Monte Carlo inversion, *Geophys J Int*, 211, 1341 – 1353, <https://doi.org/10.1093/gji/ggx355>, 2017.
- Maurya, P., Fiandaca, G., Christiansen, A., and Auken, E.: Field-scale comparison of frequency- and time-domain spectral induced polarization, *Geophys J Int*, 214, 1441 – 1466, <https://doi.org/10.1093/gji/ggy218>, 2018.
- McNeill, J.: *Electromagnetic terrain conductivity measurement at low induction numbers*, Technical note TN-6, Geonics Ltd., 1980.
- 35 Militzer, H. and Weber, F.: *Angewandte Geophysik, 2: Geoelektrik-Geothermik-Radiometrie-Aerogeophysik*, Springer Wien, Akademie-Verlag Berlin, 1985.

- Murton, J. B., Kuras, O., Krautblatter, M., Cane, T., Tschofen, D., Uhlemann, S., Schober, S., and Watson, P.: Monitoring rock freezing and thawing by novel geoelectrical and acoustic techniques, *J Geophys Res-Earth*, 121, 2309 – 2332, <https://doi.org/10.1002/2016JF003948>, 2016.
- Olatinsu, O. B., Olorode, D. O., and Oyedele, K. F.: Radio frequency dielectric properties of limestone and sandstone from Ewekoro, Eastern Dahomey Basin, *Advances in Applied Science Research*, 4, 150 – 158, 2013.
- Olhoeft, G. R.: Electrical properties of natural clay permafrost, *Can J Earth Sciences*, 14, 16 – 24, <https://doi.org/10.1139/e77-002>, 1977.
- Palacky, G. J.: Resistivity characteristics of geologic targets, In: *Electromagnetic methods in applied geophysics*, 52 - 129, <https://doi.org/10.1190/1.9781560802631.ch3>, 1988.
- Pelton, W., Ward, S., Hallof, P., Sill, W., and Nelson, P.: Mineral discrimination and removal of inductive coupling with multifrequency IP, *Geophysics*, 43, 588 – 609, <https://doi.org/10.1190/1.1440839>, 1978.
- Petrenko, V. and Whitworth, R.: *Physics of Ice*, Oxford University Press, New York, 2002.
- Przyklenk, A., Hördt, A., and Radić, T.: Capacitively-Coupled Resistivity measurements to determine frequency-dependent electrical parameters in periglacial environments - theoretical considerations and first field tests, *Geophys J Int*, 206, 1352 – 1365, <https://doi.org/10.1093/gji/ggw178>, 2016.
- Radić, T.: First Results from the New Multi-purpose Instrument CapGeo, 19th European Meeting of Environmental and Engineering Geophysics, Near Surface Geoscience, <https://doi.org/10.3997/2214-4609.20131364>, 2013.
- Routh, P., Oldenburg, D., and Li, Y.: Regularized inversion of spectral IP parameters from complex resistivity data, *Expanded Abstracts of the 68th Annual International Meeting, Society of Exploration Geophysicists*, pp. 810 – 813, 1998.
- Rowan, M.: Structural geometry of the Wildhorn Nappe between the Aar massif and the Brienzer See, *Eclogae Geol Helv*, 86/1, 87 – 119, 1993.
- Scherler, M., Hauck, C., Hoelzle, M., Stähli, M., and Völksch, I.: Meltwater infiltration into the frozen active layer at an alpine permafrost site, *Permafrost Periglac*, 21, 325 – 334, <https://doi.org/10.1002/ppp.694>, 2010.
- Seidensticker, K., Möhlmann, D., Apathy, I., Schmidt, W., Thiel, K., Arnold, W., Fischer, H., Kretschmer, M., Madlener, D., Peter, A., Trautner, R., and Schieke, S.: Sesame – An Experiment of the Rosetta Lander Philae: Objectives and General Design, *Space Sci Rev*, 128, 301 – 337, <https://doi.org/10.1007/s11214-006-9118-6>, 2007.
- Seshadri, S., Chin, K., Buehler, M., and Anderson, R.: Using Electrical Impedance Spectroscopy to Detect Water in Planetary Regoliths, *Astrobiology*, 8, 781 – 792, <https://doi.org/10.1089/ast.2007.0180>, 2008.
- Souffaché, B., Cosenza, P., Flageul, S., Pencolé, J.-P., Seladji, S., and Tabbagh, A.: Electrostatic multipole for electrical resistivity measurements at the decimetric scale, *J Appl Geophys*, 71, 6 – 12, <https://doi.org/10.1016/j.jappgeo.2010.01.009>, 2010.
- Stabbel, B.: Development of the diatom flora in Prestvannet, Tromsø, northern Norway, *Norsk Geol Tidsskr*, 65, 179 – 186, 1985.
- Stillman, D., Grimm, R., and Dec, F.: Low-Frequency Electrical Properties of Ice-Silicate Mixtures Regoliths, *J Phys Chem-US*, 114, 6065 – 6073, <https://doi.org/10.1021/jp9070778>, 2010.
- Tabbagh, A., Hesse, A., and Grard, R.: Determination of electrical properties of the ground at shallow depth with an electrostatic quadrupole: Field trials on archaeological sites, *Geophys Prospect*, 41, 579 – 597, <https://doi.org/10.1111/j.1365-2478.1993.tb00872.x>, 1993.
- Tarasov, A. and Titov, K.: On the use of the Cole–Cole equations in spectral induced polarization, *Geophys J Int*, 195, 352 – 356, <https://doi.org/10.1093/gji/ggt251>, 2013.
- Telford, W. M., Geldart, L. P., and Sheriff, R. E.: *Applied Geophysics*, Cambridge Univ. Press, 2. edn., textbook gravity seismics electrical-properties magnetics MT resistivity DC IP tellurics WL, 1990.

- Wang, Z., Wang, S., Fang, G., and Zhang, Q.: Investigation on a Novel Capacitive Electrode for Geophysical Surveys, *J Sensors*, 2016, <https://doi.org/10.1155/2016/4209850>, 2016.
- Weidelt, P.: Grundlagen der Geoelektrik, in *Handbuch zur Erkundung des Untergrundes von Deponien und Altlasten*, pp. 65-94, ed. Knödel, K., Krummel, H., Lange, G., Band 3: Geophysik, Springer, Berlin, 1997.
- 5 Weigand, M. and Kemna, A.: Relationship between Cole-Cole model parameters and spectral decomposition parameters derived from SIP data, *Geophys J Int*, 205, 1414 – 1419, <https://doi.org/10.1093/gji/ggw099>, 2016.
- Yuval, D. and Oldenburg, W.: Computation of Cole-Cole parameters from IP data, *Geophysics*, 62/2, 436 – 448, <https://doi.org/10.1190/1.1444154>, 1997.
- Zorin, N. and Ageev, D.: Electrical properties of two-component mixtures and their application to high-frequency IP exploration of permafrost, *Near Surf Geophys*, 15, 603 – 613, <https://doi.org/10.3997/1873-0604.2017043>, 2017.
- 10